Statement of contributions:

Statement of contributions to field:

While it is widely accepted that early bolting generally confers early leaf senescence, the molecular basis of this temporal relationship has not been explored. Arabidopsis shows leaf senescence related gene expression changes in older rosette leaves associated with the transition to bolting at the shoot apical meristem that may explain this relationship. This can help inform the production of crops that could overcome early leaf senescence during stress induced early-bolting. Furthermore, this study identified potential novel early regulators of leaf senescence.

Gene Expression Changes Occurring at Bolting Time are Associated with Leaf Senescence in Arabidopsis

Running title: Bolting Confers Senescence Gene Expression

Will E Hinckley[1]*, **Judy A. Brusslan[2]**
[1]Department of Biology, New York University, New York, NY, 10003, USA
[2]Department of Biological Sciences, California State University, Long Beach, Long Beach, CA 90840-9502, USA
*Corresponding Author
weh6454@nyu.edu

Keywords: Flowering Time, Leaf Senescence, Development, Transcriptomics, Stress, Bolting, Arabidopsis trithorax

Abstract:

In plants, the vegetative to reproductive phase transition (termed bolting in Arabidopsis) generally precedes age-dependent leaf senescence (LS). Many studies describe a temporal link between bolting time and LS, as plants that bolt early, senesce early, and plants that bolt late, senesce late. However, the molecular mechanisms underlying this relationship are unknown and are potentially agriculturally important, as they may allow for the development of crops that can overcome early LS caused by stress-related early phase transition. We hypothesized that gene expression changes associated with bolting time were regulating LS. We used a mutant that displays both early bolting and early LS as a model to test this hypothesis. An RNA-seq time series experiment was completed to compare the early bolting mutant to vegetative WT plants of the same age. This allowed us to identify bolting time-associated genes (BAGs) expressed in an

older rosette leaf at the time of inflorescence emergence. The BAG list contains many well characterized LS regulators (*ORE1, WRKY45, NAP, WRKY28*), and GO analysis revealed enrichment for LS and LS-related processes. These bolting associated LS regulators likely contribute to the temporal coupling of bolting time to LS.

Introduction:

Leaf senescence (LS) is the sequential death of older leaves, one-by-one, as the plant matures, while whole plant senescence is the simultaneous death of all leaves at the end of the growing season in monocarpic species (Nooden et al., 1997). A visual hallmark of LS is leaf yellowing, caused by chlorophyll degradation (Ougham et al., 2008; Tamary et al., 2019). During these processes, nitrogen (most commonly in the forms of nitrate, asparagine, and glutamine) and other macromolecules are recycled from dying leaves (sources) and relocated to growing tissues (sinks), including the reproductive organs (Havé et al., 2017). A better understanding of the regulation of LS may have important agricultural implications on yield and nutrition content.

Endogenous signaling molecules that control LS have been well characterized. Ethylene, abscisic acid (ABA), jasmonic acid (JA), salicylic acid (SA), and reactive oxygen species (ROS) are known to promote both age dependent and/or dark induced LS (Jing et al., 2005; Khanna-Chopra, 2012; Yuehui et al., 2002; K. Zhang et al., 2013; Zhao et al., 2017). Many genetic and epigenetic regulators of LS have also been identified. (Nicole Ay, Bianka Janack, 2014; Woo et al., 2019). Tri-methylated Lysine 4 on Histone 3 (H3K4me3) is an active gene expression mark associated with increased expression of many LS related genes (Brusslan et al., 2015; P. Liu et al., 2019). Histone Deacetyltransferase 6 (HDA6) regulates both flowering time and LS (Keqiang Wu, Lin Zhang, Changhe Zhou, Chun-Wei Yu, 2008). POWERDRESS interacts with HDA9 to promote aging (X. Chen et al., 2016). The H3K27me3 demethylase REF6 was also shown to promote leaf senescence (X. Wang et al., 2019). H3K9 acetylation via HAC1 (HISTONE ACETYLTRANSFERASE-1) promotes LS, and the transcription factor (TF) ERF022, a potential HAC1 target, positively regulates LS (Hinckley et al., 2019). Other individual TFs have been shown to regulate LS, for example *NAP, WRKY53, WRKY75,* and *ORE1* are positive regulators and JUB1, WRKY54 and WRKY70 negatively regulate LS (Guo et al., 2017; Lei et al., 2020; Miao et al., 2004; Qiu et al., 2015; Zentgraf & Doll, 2019). There are multiple large TF families that are associated with age dependent and dark induced LS (*WRKY, NAC, ERF*) (Bakshi & Oelmüller, 2014; Jiang et al., 2017; H. J. Kim et al., 2016; Koyama et al., 2013; Koyama, 2014; Li et al., 2018). Furthermore, stress, defense, and LS signaling overlap and some TFs are known to bridge stress and LS signaling (*SAG113, NAP, WRKY53*) (Asad et al., 2019; Nir Sade, María del Mar Rubio-Wilhelmi, Kamolchanok Umnajkitikorn, 2018; Woo et al., 2013).

While many regulators have been identified that function at the onset of or during LS, less is known about developmentally early regulators of LS. Kim et al. recently uncovered the NAC troika, consisting of three Arabidopsis NAC TFs that act in young rosette leaves to prevent early LS (H. J. Kim et al., 2018). To our knowledge, this represents the earliest known regulation of LS in Arabidopsis. Still, greater knowledge of developmentally early regulators of LS is needed to better optimize its timing.

Preceding LS is the vegetative to reproductive phase transition, which in Arabidopsis is termed bolting or flowering: the development of the primary inflorescence that produces cauline leaves, inflorescence meristems, and floral meristems. Many different environmental and

autonomous cues can induce flowering independently, however all pathways converge on conserved master flowering time regulators: FT, SOC1, and FLC (Mouradov et al., 2002; Song et al., 2018). Stress can also induce flowering (Kiyotoshi Takeno, 2016; Wada & Takeno, 2010). The function of stress signaling in both flowering time and LS may serve as a link that allows reproductive success during biotic or abiotic stress.

A classic study in Arabidopsis showed LS in the fifth and sixth leaves was similar in WT and two late flowering mutants, *co-2* and *fca*, suggesting that leaf age was an important determinant of LS, not the vegetative-reproductive phase transition. Furthermore, LS was unaffected in male sterile (*ms1-1*) mutants, indicating that seed development did not influence LS (Hensel et al., 1993).

Other studies in Arabidopsis, however; show a relationship between the timing of bolting and leaf and/or whole plant senescence. Two ecotypes, Ler and Cvi, showed a negative correlation between bolting and sixth leaf longevity; Ler bolted much later and displayed shorter leaf longevity than Cvi (Luquez VM, Sasal Y, Medrano M, Martín MI, Mujica M, 2006). A similar study using more conventional quantitative methods of LS looked at the relationship between the natural bolting times and LS phenotypes of multiple Arabidopsis ecotypes, and found the opposite result of Luquez et al. Bolting age positively correlated to the chlorophyll content of the five largest leaves (measured at 59 DAS) among eight ecotypes, with later bolting ecotypes having more chlorophyll, implying a delay in LS. In addition, these eight ecotypes revealed a negative correlation between bolting age and percent yellow leaves in the rosette; here later bolting ecotypes had a smaller percentage of senescent leaves (Balazadeh et al., 2008). These findings show that the earlier bolting ecotypes were further progressed into leaf and whole plant senescence than later bolting ecotypes, indicating the timing of LS is related to the bolting time of each individual ecotype. However, these studies are based on the bolting times of each ecotype and do not address the effects of altered bolting time within one ecotype.

A similar positive correlation between bolting age and both leaf and whole plant senescence was seen in a single ecotype model. *KHZ1* and *KHZ2* encode highly similar KH domain-Zn finger proteins. *khz1 khz2* double mutants bolt late and show delayed leaf and whole plant senescence. Overexpression of either KHZ1 or KHZ2 resulted in early bolting, leaf and whole plant senescence (Yan et al., 2017). Here, a positive correlation was seen between the varying bolting times and LS phenotypes in one ecotype. Some genes have been identified that regulate both flowering time and LS in Arabidopsis (*SOC1, WRKY75*), which may partially explain this temporal relationship in the single ecotype model (J. Chen et al., 2017; L. Zhang et al., 2018).

Although there are conflicting data, most recent studies point to a positive correlation between bolting and leaf and whole plant senescence. We hypothesized that there are gene expression changes occuring in the rosette associated with the reproductive transition at the shoot apical meristem that regulate LS. These gene expression changes could be contributing to the positive correlation seen between bolting time and LS. To address this hypothesis, we isolated a mutant that displays both early bolting and early LS. We then completed an RNA-seq time series experiment that compared the early bolting mutants to vegetative WT plants of the same age. Our approach allowed the identification of leaf gene expression changes specifically associated with bolting time. This list of 398 Bolting Associate Genes (BAGs) was enriched for LS and LS-related GO terms, and includes many well characterized LS regulators. Using a LS database (Li, Yang Zhang, Dong Zou, Yi Zhao, Hou-Ling Wang, Yi Zhang, Xinli Xia, Jingchu Luo, Hongwei Guo, 2020), we found that 202 of these BAGs are known to be associated with LS. A list of

potential novel early LS regulators was proposed. We then produce a gene regulatory network summarizing BAG interactions generated from publicly available DAP-seq TF binding site data (O'Malley et al., 2016). This study shows that there are leaf gene expression changes associated with bolting that may regulate LS in *Arabidopsis thaliana.* These early regulators of LS likely contribute to the temporal relationship connecting bolting time and LS.

Results:

atx Triple Mutant Phenotype

Previous data show that changing levels of the H3K4me3 mark correlate to changes in gene expression during age-dependent developmental LS (Brusslan et al., 2015). The peak of H3K4me3 marks in Arabidopsis is located about 400 bp downstream of the transcription start site (TSS) and is correlated to high expression of the nearby gene (Z. Zhang et al., 2016). For 389 genes, H3K4me3 marks increased in parallel with gene expression during age-dependent LS, and we named these genes H3K4me3-Senescence Up-Regulated Genes (K4-SURGs). We initially hypothesized that H3K4me3 accumulation might be a mechanism for increasing expression of senescence related genes. To address this hypothesis, we generated H3K4me3 methyltransferase mutants and studied their LS phenotypes.

Class III Arabidopsis trithorax (*ATX)* histone methyltransferases methylate H3K4 (Pontvianne et al., 2010). Different *ATX* enzymes catalyze different methyltransferase activities (mono-, di-, tri-methylation), and some single mutants display more severely altered developmental phenotypes than others (L. Q. Chen et al., 2017; Tamada et al., 2009; Yun et al., 2012). Our single *atx1*, *atx3*, and *atx4* mutants and double mutant combinations did not display a detectable change in LS, leading to the isolation of a homozygous *atx* triple mutant (*atx1 atx3 atx4*). We isolated two *atx* triple mutants (TM1 and TM2), which contain the same alleles but are derived from different F populations from distinct individual parents, thus are independent isolates of the same genotype. The (*atx1 atx3 atx4)* triple mutant genotype was confirmed both by PCR and RT-PCR (Supplemental Data File 1).These mutants displayed significantly early bolting (Figure 1A) and significantly early LS, quantified by *NIT2* and *WRKY75* mRNA induction (Figure 1B-C) and by chlorophyll loss (Figure 1D). We also confirmed that early bolting translated to an early flowering phenotype (Supplemental Data File 2, Sheet_5), meaning bolting is an appropriate phenotype marker for the vegetative-reproductive transition. The accumulation of H3K4me3 downstream of the *FLOWERING LOCUS C (FLC)* TSS is associated with high expression of *FLC*, a flowering inhibitor, thereby preventing the vegetative to reproductive transition (bolting)(Pien et al., 2008; Yun et al., 2012). The early bolting phenotype in the *atx* TMs is likely due to a decrease in H3K4me3 accumulation at the *FLC* locus and decreased gene expression of this and related flowering inhibitors.

NIT2 encodes a nitrilase and is a robust K4-SURG that serves as an mRNA marker for LS (Brusslan et al., 2012). *WRKY75* is a well characterized positive regulator of LS (T. Kim et al., 2019) that was also identified as a K4-SURG. H3K4me3 is an activating mark, thus if hypomethylation caused by *atx* mutation affected *NIT2* or *WRKY75,* we would expect lower gene expression, but we detected the opposite (Figure 1B-C). This led us to hypothesize that *NIT2* and *WRKY75* induction were not caused by local H3K4me3 changes, rather the coupling of LS to bolting time might be responsible. The genetic mechanism behind this temporal relationship has not been defined, and it became our goal to identify gene expression changes associated with the bolting event that may be regulating LS.

RNA-seq Time-Series Experimental Design

We completed an RNA-seq time-series experiment that compared the early bolting *atx* TMs to vegetative WT Col-0 plants of the same age over a six-day time course (Figure 2). This single ecotype approach overcomes the genetic variability in different Arabidopsis ecotypes and the confounding factor of ecotypes that are acclimated to different geographical parts of the world being grown in a single environment. If LS-related signaling was being initiated in leaves by bolting, we would expect to see senescence-related differentially expressed genes (DEGs) between the *atx* TMs and WT, and enrichment of senescence-related biological processes within these DEGs.

Plants that bolted at the peak of *atx* TM bolting (Day 24-25, T0) were grouped. Plants were then randomly selected from this group for leaf 6 harvesting, which began at T0 and continued in two day increments (T2, T4, and T6). This synchronization to bolting ensured the plants were developmentally similar. Vegetative WT leaf 6 control tissue was harvested at the same time points. This design allowed us to differentiate gene expression changes associated with bolting versus those associated with age. cDNA libraries were prepared and subject to high-throughput sequencing (Supplemental Data File 3 reports FPKM values).

As expected, hierarchical transcriptome clustering showed TM1 and TM2 are highly similar at each time point (Figure 3A). All T0 samples clustered together, regardless of genotype, because they are developmentally the most similar. The T2, T4, and T6 transcriptomes from bolting *atx* TMs cluster away from the vegetative WT samples (T0 and T2). WT samples from T4 and T6 cluster with the *atx* TM bolting samples, likely because they are nearing the vegetative-reproductive transition. These clustering patterns were also seen using Principal Component Analysis (PCA, Figure 3B).

RNA-seq Data Analysis Strategy

Three methods were used to determine differential expression. A gene needed to be identified by at least two different statistical methods to be considered a DEG. A (Genotype + Time + Time:Genotype) design was used to run an LRT test with (~Time) as a reduced model in DESeq2, which treated time as a continuous variable and removed genes that show the same expression change over time in all samples (Love et al., 2014). edgeR was used to compare each mutant to WT separately at each time point, meaning time was treated as a factor (Mark D. Robinson, Davis J. McCarthy, 2009). Lastly, a T-test based method was written in R (All code used for differential expression analysis can be found in Supplemental Data File 4). The use of multiple methods increased stringency to prevent spurious detection of differential gene expression. Our list of 750 DEGs (Supplemental Data File 5, Sheet 3) contained many bolting/flowering time regulators (*SOC1, FT, MED18, FLC, FPA, CIB1, CIB5 , SEP1, SEP3, MAF4, and MAF5*), providing confidence that our harvesting method and differential expression analysis isolated bolting related gene expression changes.

We then sought to validate these results in WT Col-0 plants undergoing the normal (not early) vegetative-reproductive phase transition in other datasets (Supplemental File 5, Sheet 4). While not synchronized to bolting, Breeze *et al.* completed a similar developmental time series experiment in Arabidopsis (Breeze et al., 2011). Leaf 7 was harvested from WT Col-0 in two day increments. We selected the time point at which plants began to flower in their time series (Day 21) and included the three subsequent time points. DEGs from these four time points were overlapped with our DEG list. Gaudin *et al.* identified genes downstream of FT and SOC1 by monitoring transcriptome changes in WT Col-0 Arabidopsis plants as they transitioned from

short day (SD) to long day (LD) photoperiods (Gaudin et al., 2019). This photoperiodic transition induces flowering, and while their transcriptomes were generated from pre-bolting plants, the genetic changes associated with the SD-LD transition are related to bolting.

Compared to our experiment, plants in these two experiments were solely WT genotypes, were not developmentally synchronized, were grown in different chambers, and DEG lists were generated using different statistical methods. However, all datasets covered the vegetative-reproductive transition. It is important to note that *FT* and *SOC1* were both found to be differentially expressed in all three experiments, indicating that canonical flowering time-related gene expression was occurring in each dataset.

Bolting Associated Genes (BAGs)

In order to be considered a bolting-associated gene (BAG), a gene had to be identified by at least two out of the three statistical methods used in our analysis, and it had to be validated in at least one of the WT time series experiments. Default parameters on Genesect from VirtualPlant 1.3 were used to determine that all gene lists displayed significant overlap (p<.001) (Katari et al., 2010). Genes identified in our experiment that did not overlap with the WT experiments may be false positives or may be specifically associated with early flowering or changes in H3K4me3 accumulation. This approach stringently identified 398 genes that are differentially expressed at bolting time (Supplemental Data File 5, Sheet 5).

A script was written in R to visualize the expression profiles of all 398 BAGs. (Supplemental Data File 6). Select gene expression profiles are shown along with the corresponding profiles from the WT time-series experiments (Figure 5). *WRKY45* increased over time in all samples except for the vegetative WT control in our experiment. *DTX50* also showed strong induction in each experiment, though it decreased back to basal levels after four days, indicating a more transient expression. *PSK4* increases at T0 and then maintains expression levels higher than WT at all subsequent time points, which corresponds to the clear induction of *PSK4* in both WT time series. *SAG20* did not show as clear of a trend of expression over time, but it was consistently higher than vegetative WT levels. *SAG20* increases expression in both WT time series. *ANT* appears to decrease expression in all datasets undergoing the vegetative reproductive transition. WT follows the same trend, with a delayed decrease in *ANT* expression compared to the *atx* TMs, likely as WT was nearing bolting time.

The 398 BAGs are enriched for both LS and LS-related biological processes (Figure 6A). The Panther Gene Ontology analysis allows extraction of the input DEGs associated with each enriched term (Huaiyu Mi, Anushya Muruganujan, 2012; Thomas et al., 2003)(Supplemental Data File 7). We intersected these input BAGs associated with individual enriched GO terms with the times that they were differentially expressed in our time series experiment (in TM2 from the edgeR analysis). We found that on average, among the genes associated with enriched GO terms, there was a significantly higher proportion of BAGs differentially expressed at T2 compared to all other time points (Figure 6B). This indicates that the BAGs associated with enriched GO terms change expression more frequently at T2, two days after bolting. These genes associated with enriched GO terms were changing at the time point most closely following the emergence of the bolt, supporting the hypothesis that the initial elongation of the bolt is the stimulus of LS-related signaling. This is further supported by the heatmap showing that the most dramatic differences in BAG expression between the *atx* TMs and WT are seen between T0 and T2 (Figure 6C). Furthermore, Short Time-series Expression Miner (STEM) clustering analysis was completed to determine if TM1 and TM2 displayed similar BAG gene expression patterns.

STEM identified mostly the same significant gene expression clusters in both mutants (Figure 6D) (Ernst & Bar-Joseph, 2006).

Potential Novel Early Regulators of LS

We then wanted to identify genes within the BAG list that either regulate or are associated with LS. Zhang *et al.* generated a database of genes known to be associated with LS (LSD 3.0)(Zhonghai Li., 2019). Using VirtualPlant, we found a significant overlap between BAGs and LSD 3.0 (p<.001). 202 of the 398 BAGs (50.7%) were shared (Supplemental Data File 5, Sheet 6). While some of these known LS-associated BAGs likely contribute to the coupling of LS to flowering time, we also wanted to find potential novel LS regulators. Kim et al completed a dark-induced detached leaf senescence (DILS) RNA-seq time series experiment with WT Col-0 plants that we used to find genes that change expression during DILS (GSE99754) (Jeongsik Kim, Su Jin Park, Il Hwan Lee, Hyosub Chu, Christopher A Penfold, Jin Hee Kim, Vicky Buchanan-Wollaston, Hong Gil Nam, Hye Ryun Woo, 2018). We compared gene expression from T0 (before dark treatment) and T3 (3 days into dark treatment) using DESeq2 with default parameters and standard cutoffs (P<0.05, FDR<0.05, and a log2 fold change>2) (Supplemental Data File 5, Sheet 7). We intersected the DILS DEGs with the BAG and LSD gene lists, and a significant overlap was found (p< 0.001). 91 BAGs were shared in the DILS experiment, but were not in the LSD (Figure 7A, Supplemental Data File 5, Sheet 8). 68 (74.7%) of these 91 genes were downregulated during *atx* TM bolting and DILS, while 15 (16.5%) were upregulated during *atx* TM bolting and DILS. Seven of these 91 genes were upregulated in bolting *atx* TMs, but downregulated during DILS and one gene was downregulated during *atx* TM bolting, but upregulated during DILS. A subset of BAGs that change expression during DILS, but are not present in the LSD, are signaling molecules that may represent novel early regulators of LS (Figure 7B).

Bolting Associated Gene Regulatory Network (GRN)

We sought to identify genetic interactions between BAGs, of which many are transcription factors (TFs). Recently, the development of DNA-Affinity-Purification sequencing (DAP-seq) has allowed for high throuput screening for TF binding sites (Bartlett et al., 2017). We wrote a script that uses DAP-seq data from GEO to generate lists of bound targets for the bolting associated TFs for which data were available. (GSE60141) (Supplemental Data Files 8 and 9)(O'Malley et al., 2016). We then intersected these data with the time and direction of differential expression from our experiment, and annotation in the LSD (Supplemental Data File 10). These data were uploaded to Cytoscape for visualization (Shannon et al., 2003). To reduce network density, nodes are only shown at the first time they were differentially expressed. A side effect of the display is that some interactions appear reversed in time. An example of this is with ANAC046 regulating *ERF054*. *ANAC046* is differentially expressed at T2, but *ERF054* is differentially expressed at every time point. Since ERF054 is only shown at T0, the first time it is differentially expressed, it appears that ANAC046 is conferring temporally backwards regulation.

All nodes in the network are BAGs. The network shows that there are bolting time associated TFs that can bind and might explain the differential expression of BAGs. There appears to be a shift from upregulation (red) to downregulation (blue) from T0 to T6. While most of the TFs appear to act independently, some interactions between TFs were identified in the DAP-seq data. *ERF054* is bound by ORE1, ANAC046, and GBF3 while *ANAC046* is bound by

HB34. Select signaling molecules were included in the subnetwork focusing on ERF054 (Figure 9). All TFs in the subnetworks confer differential expression at multiple time points and have both shared and independent targets.

DAP-seq binding data show multiple senescence associated TFs (ORE1, ANAC046, HB34, and GBF3) converging towards *ERF054*. This may explain the gene expression profile of *ERF054*, both in our experiment and Breeze et al. (Supplemental Data File 6, At4g28140). Note that time resolution of data are not shown in the subnetworks. Only *ORE1* binds to *ERF054* at T0, explaining the significantly increased expression of *ERF054* at T0 in the *atx* TMs relative to WT. However, even greater induction of *ERF054* gene expression is seen in the *atx* TMs at T2 relative to WT, when other TFs (*GBF3, ANAC046,* and *HB34*, which itself binds *ANAC046*) are differentially expressed and can also bind to *ERF054*. This network also shows that many targets of these TFs are differentially expressed in DILS but not included in the LSD (white nodes with red labels). These data further support these genes being novel LS regulators, as they are directly bound by well characterized LS-promoting TFs.

Other subnetworks were created by selecting known TFs known to confer LS-related signaling: WRKY45 (Figure 10A) and HB34 (Figure 10B). WRKY45 is a positive regulator of LS (L. Chen et al., 2017) that increases expression at the time of bolting (Figure 5). *WRKY45* expression is induced during DILS, and it is present in the LSD. The subnetwork shows WRKY45 binds to many LS-associated genes (grey nodes), and many genes that are differentially expressed during DILS (nodes labeled in red). For example, WRKY45 binds to *AHK4,* which is downregulated at bolting and is a negative regulator or LS (Riefler et al., 2006). This interaction supports WRKY45 being a positive regulator of LS. WRKY45 also binds to genes that are differentially expressed during DILS, but are not present in the LSD (white nodes with red labels). The same is seen for HB34. HB34 binds and may activate the expression of *ANAC046*, a positive regulator of LS (Oda-Yamamizo et al., 2016). It also binds to known SAGs and potential novel regulators of LS. Interestingly, most of the potentially novel LS regulators are downregulated in the subnetworks (Figures 9 and 10: *CIA2, DWF1, RKL1, CMCU, BZIP34, RLK902*).

Discussion

The goal of our study was to better understand the molecular connection between the vegetative-reproductive transition and LS. We hypothesized that there are LS-related gene expression changes associated with the bolting event. Using RNA-seq, we generated a list of 398 bolting associated genes (BAGs). 202 of these BAGs were present in the Leaf Senescence Database (LSD), some of which are likely responsible for temporally connecting LS to bolting time. We also identified 91 BAGs that are differentially expressed during dark-induced leaf senescence (DILS) but are not present in the LSD. Further study of these 91 genes may reveal that some are novel early regulators of LS.

atx Triple Mutant Phenotypes

While the two *atx* triple mutants (TM1 and TM2) contain the same *atx1 atx3* and *atx4* alleles, we feel justified in treating them as two independent early flowering mutants: TM2 appears to have a stronger early LS phenotype, it consistently produced more DEGs than TM1, and clustered further away from WT than TM1 did in PCA analysis (Figure 3B). We think that by overlapping the results between TM1 and TM2, we reduced the probability of false

discoveries. Furthermore, TM2 consistently displayed a slightly more severe early LS phenotype than TM1 (Figure 1D, Supplemental Data File 2). There are likely background mutations unique to TM1 or TM2 that contribute to this difference. Regardless, all BAGs were significantly differentially expressed in both TM1 and TM2. Early flowering has been reported in other *atx* mutants (Berr et al., 2015; Yun et al., 2012) which is consistent with our findings. Chen et al isolated an (*atx3, atx4, atx5)* triple mutant but did not report a change in flowering time or LS (L. Q. Chen et al., 2017). The five *ATX* enzymes are classified into two clades (*ATX1* and *ATX2*), and (*ATX3, ATX4*, and *ATX5)*, thus their genetic divergence may explain the difference in phenotypes between the (*atx1 atx3 atx4*) and the (*axt3 atx4 atx5*) triple mutants.

RNA-seq Time Series Experiment

Synchronizing tissue harvesting to bolting differentiated bolting-associated and age-associated changes in gene expression. Multiple statistical approaches were used for the identification of 750 initial DEGs since there is not one perfect statistical approach for our time-series analysis. Treating time as a continuous variable as we did in DESeq2 helps to identify time-resolved gene expression changes. However, our edgeR based method treated time as a factor, which may have allowed greater detection of transient changes in gene expression. It is common to see high overlap between edgeR and DESeq2, however that typically occurs when the same underlying statistical design is used. Here, we did not expect strong overlap as the programs were run with different designs. Even with the varying designs, Genesect found significant overlap between these gene lists (p< 0.001).

Lack of reproducibility for large dataset analysis is a chronic issue (Joël Simoneau, Simon Dumontier, Ryan Gosselin, 2019; Porra et al., 1989). While some programs are commonly used for differential expression analysis (edgeR, DESeq2, limma), we felt justified to include a T-test method, as it increased transparency and showed that a bulk of the DEGs identified by the two commonly used programs were supported by simple T-tests. Our stringent overlapping method should reduce the risk of false positives.

It was also important to validate our results in WT plants because the *atx* TMs may have unknown epigenetic effects. It would have been ideal to repeat the RNA-seq time-series experiment, but to center it around bolting WT plants, and use early and late flowering controls, however our use of publicly available data was more practical and cost effective. While this is one limitation to our study, two published experimental designs were similar to ours. These two WT datasets used similarly aged leaves, similar time resolution, and were centered around the vegetative-reproductive transition, which was made apparent by the identification of *FT* and *SOC1* as DEGs in both. As expected, our dataset had stronger overlap with Breeze *et al.* than Gaudin *et al.*, as plants in the Breeze *et al.* dataset were bolting. Gaudin *et al.* was specifically looking at the genetic changes associated with *FT* and *SOC1* expression, and their plants were not yet bolting. Both datasets had multiple replicates for high confidence output. Ultimately, changes in gene expression will need to be validated with real-time qPCR of separate biological replicates.

Bolting Associated Genes (BAGs)

The 398 BAGs were enriched for LS and LS-related biological process GO terms. This supports the hypothesis that bolting stimulates LS- related signaling. The following known LS-associated genes were identified in our *atx* triple mutant analysis and then further validated in **both** WT time series experiments. *SOC1* is a classic example of a gene that positively regulates

both flowering time and LS (J. Chen et al., 2017). *ANAC032* positively regulates flowering time and LS and is responsive to oxidative stress (Mahmood et al., 2016). *WRKY45* positively regulates LS, and WRKY45 overexpression lines displayed early bolting along with early LS, suggesting WRKY45 may play a role in regulating both flowering time and LS (L. Chen et al., 2017). *SAG20* and *SEN1* are both LS marker (Fernández-Calvino et al., 2016; Schenk et al., 2005; Weaver et al., 1998). *DEAR1* promotes cell death and SA synthesis (Tsutsui et al., 2009). Mutation of *ELS1*, a close homolog of the BAG *DTX50* results in both early flowering and early LS (Z. Wang et al., 2016). *DTX50* is a transiently expressed ABA transporter (H. Zhang et al., 2014). The induction of *DTX50* at bolting time in all experiments indicates ABA flux is associated with bolting, which could be promoting LS. *ADP7 (SSPP)* is a senescence suppressed protein phosphatase (Xiao et al., 2015). Some genes identified in all three experiments were also found to be K4-SURGs (*WRKY45*, mate efflux AT1G33110, peroxidase superfamily protein At2g371300, *BGLU11, CAX3, CTPS4, PSK4,* and *TBL38* (Brusslan et al., 2015).

Other LS related BAGs were shared between the *atx* TMs and Breeze *et al.* dataset. *ORE1* (*ANAC092*) is a well studied promoter of LS (Qiu et al., 2015). *WRKY28* is responsible for activating SA biosynthesis genes and promotes LS (Tian et al., 2020; van Verk et al., 2011). *SAG13* is a ROS responsive BAG that regulates DILS (Dhar et al., 2020). When knocked out in higher order mutants to reduce redundancy with other CRF TFs, *crf2* mutants showed delayed LS, suggesting the BAG *CRF2* works with other CRF TFs to promote LS (Raines et al., 2016). *BOI* attenuates cell death and regulates flowering time (Nguyen et al., 2015). BHLH112 plays roles in both flowering time and stress response (H. C. Chen et al., 2017; Y. Liu et al., 2015). The following genes were shared between the atx TMs and the Gaudin et al dataset. *WRKY46* is responsible for activating SA biosynthesis genes and promotes LS (van Verk et al., 2011). *WRKY48* is a stress and pathogen induced regulator of plant defense. (Deng-Hui et al., 2008). The BAG *SAUR41* acts redundantly with *SAUR49* to promote LS by regulating *SSPP*, another BAG with a known role in LS (Wen et al., 2020; Xiao et al., 2015).

Other BAGs associated with flowering time, seed development, and seed nutrient content were also identified. *UMAMI28* is responsible for transporting amino acids to the developing seeds (Müller et al., 2015). *SUS3* regulates sugar metabolism in developing seeds (Angeles-Núñez & Tiessen, 2010). The BAG *SEP1* works redundantly with *SEP2* and *SEP3* to regulate flower and ovule development (Pelaz et al., 2000). *CURVY1* regulates both flowering time and seed development (Gachomo et al., 2014). *FUL (AGL8)* and *BFT* regulate flowering time (Marian Bemer, Hilda van Mourik, Jose M Muiño, Cristina Ferrándiz, Kerstin Kaufmann, 2017; Ryu et al., 2011; Vicente Balanzà, Irene Martínez-Fernández, 2014). These genes change expression in the 6th rosette leaf, suggesting they may contribute to processes other than flower and seed development and nutrition.

The abundance of enriched genes peaking at T2 supports our hypothesis that bolting stimulates LS signaling. Significantly more genes associated with enriched processes were differentially expressed two days after the bolting event. The heatmap (Figure 6C) also highlights the most differential expression in TMs relative to WT between T0 and T2. Furthermore, half of the BAG list was found to be in the LSD, meaning half of the BAGs are known to be associated with LS. These findings further support that the bolting event stimulates LS related signaling in mature leaf 6, and that our harvesting method captured the signaling stimulated by bolting.

Potential Novel LS Regulators

Ninety-one BAGs were not present in the LSD, but were differentially regulated during DILS (Figure 7B). A majority of the potential novel LS regulators (91%) change expression in the same direction during both bolting and DILS, but seven (7.7%) are upregulated at bolting and downregulated during DILS. These seven genes might prevent LS prior to and during bolting, and then must be downregulated for normal or dark-induced LS to proceed. Only one gene was downregulated in bolting *atx* TMs but upregulated during DILS. Some of these 91 genes regulate processes that are known to be related to LS. For example, *ORA47* regulates both ABA and JA synthesis (H. Chen et al., 2016). The BAG BZIP34 forms heterodimers with BZIP61, which is a BAG in the LSD that is also differentially expressed during DILS (Gibalová et al., 2009)(LSD database annotation). BZIP61 and BZIP34, which share 71% amino acid identity, may work together to regulate LS downstream at bolting time. While many of these 91 genes have known functions related to LS, a phenotype screen of verified mutants is needed to support their function.

GRNs

The main GRN (Figure 8) shows that BAG TFs can regulate the expression of other BAGs at every time point in our experiment. This format was obtained by separating TFs and targets. Nodes were then separated by time. Some targets were removed from the subnetworks to reduce density, however no genes that were differentially expressed during DILS (red labels) or were potential novel LS regulators (red labels on white nodes) were removed. Subnetworks (Figures 9 and 10) show how individual TFs have the potential to regulate many well known regulators of development and LS. CML47 inhibits SA accumulation and defense, thus the upregulation of CML47 at bolting may serve as a mechanism to prevent inappropriately early LS (Lu et al., 2018). NAP is a positive regulator of LS, thus its decrease in expression at bolting may also be working to prevent early LS (Lei et al., 2020). *HAI1 (SAG113)* is ABA responsive and is downstream of NAP (Wong et al., 2019; K. Zhang & Gan, 2012). KMD2 inhibits CK signaling, which delays LS, thus the induction of KMD2 at the time of bolting might promote LS (H. J. Kim et al., 2013). *NIA1* and *NIA2* are responsible for nitrate reduction in plants and were both significantly upregulated after bolting time (Olas & Wahl, 2019). N metabolism and transport are a major component of LS. Both *NIA1* and *NIA2* are bound by many well characterized LS regulators that change expression at bolting time (Figures 9 and 10).

Conclusion

We have identified 398 BAGs expressed in mature leaf 6 that change expression at the time of bolting. 202 of these BAGs are known to be associated with LS (Zhonghai Li et al., 2020). Many of these BAGs are also differentially expressed during DILS. Furthermore, we identify a set of genes that change expression during bolting and DILS, but are not in the LSD, meaning some may be novel early regulators of LS. Together, this study identifies LS-related gene expression changes that occur in a specific mature rosette leaf two days after the vegetative to reproductive transition at the shoot apical meristem.

Abbreviations
ABA- abscisic acid
BAGs- Bolting Associated Genes
CK- Cytokinin
DEG -Differentially Expressed Genes

DILS- Dark Induced Leaf Senescence
GEO - Gene Expression Omnibus
GO - Gene Ontology
GRN- Gene Regulatory Network
JA- Jasmonic acid
LS- Leaf Senescence
LSD- Leaf Senescence Database
PCA- Principal Component Analysis
PCR- Polymerase Chain Reaction
RT-PCR- Reverse Transcriptase Polymerase Chain Reaction
qPCR -Quantitative Polymerase Chain Reaction
SA- Salicylic Acid
T0- Bolting Time
T2- 2 Days After Bolting
T4- 4 Days After Bolting
T6- 6 Days After Bolting
TMs- *atx* Triple Mutants
WT - Wildtype

Materials/Methods

Plant growth conditions

Arabidopsis thaliana plants were grown in Sunshine® Mix #1 Fafard®-1P RSi soil (Sungro Horticulture), which was treated with Gnatrol WDG (Valent Professional Products) (0.3 g/500 ml H_2O) to inhibit the growth of fungus gnat larvae. Plants were sub-irrigated with Gro-Power 4-8-2 (Gro-Power, Inc., 8 ml per gallon), and grown in Percival AR66L2X growth chambers under a 20:4 light:dark diurnal cycle (Long Day) with a light intensity of 28 μmoles photons m^{-2} s^{-1}. The low light intensity prevents light stress in older leaves, which was evident as anthocyanin accumulation at higher light intensities. To compensate for the reduced light intensity, the day length was extended. The petiole of the sixth leaf to emerge was marked with a thread on individual plants.

Genotype Analysis

Genomic DNA was isolated from two-three leaves using Plant DNAzol Reagent (Thermo Fisher) following manufacturer's instructions. Pellets were dried at room temperature for at least two hours, and resuspended in 30 μl TE (10 mM Tris, pH 8.0, 1 mM EDTA) overnight at 4°C. One microliter of genomic DNA was used as a template in PCR reactions with primers listed in supplemental file 1. All standard PCR reactions were performed with a 57°C annealing temperature using *Taq* polymerase with Standard *Taq* Buffer (New England Biolabs).

Chlorophyll Analysis

One hole-punch was removed from each marked or detached leaf and incubated in 800 µl N,N-dimethyl formamide (DMF) overnight in the dark. 200 µl of sample was transferred to a quartz microplate (Molecular Devices) and absorbance at 664 and 647 nm was measured with a BioTek Synergy H1 plate reader. Absorbance readings were used to determine chlorophyll concentration (Porra et al., 1989). For each genotype/condition, $n = 6$ single hole punches from 6 individual plants.

Gene Expression

Total RNA was isolated from leaf 6 using Trizol reagent. 1,000 ng of extracted RNA was used as a template for cDNA synthesis using MMLV-reverse transcriptase (New England Biolabs) and random hexamers to prime cDNA synthesis. The cDNA was diluted 16-fold and used as a template for real-time qPCR using either ABsolute QPCR Mix, SYBR Green, ROX (Thermo Scientific) or qPCRBIO SyGreen Blue Mix Hi-Rox (PCR Biosystems), in Step One Plus or Quant Studio 6 Flex (Thermo Fisher) qPCR machines. All real-time qPCR reactions were run with a 61°C annealing temperature, and normalized to *ACT2*.

RNA-seq library construction

Ten plants, per line at each time point were selected for harvesting from the developmentally synchronized group of bolting plants. Leaf 6 was harvested from all 10 plants and immediately flash-frozen together. A mortar and pestle were used to grind tissue in liquid nitrogen. Homogenized tissue was separated evenly into three tubes to be treated as three replicates. The Breath-Adaptive Directional sequencing (BrAD-seq) (Townsley et al., 2015) protocol was completed to generate cDNA libraries. A 1/50ᵗ dilution of the final library was used with *ACT2* primers in qPCR to check for library consistency. The Illumina-ready cDNA libraries that were then sequenced at the UCI Genome High-Throughput Facility (GHTF).

RNA-seq data analysis

Raw data were aligned to the TAIR10 genome and counted using Kallisto. Data were then exported to R and rounded to the nearest integer for differential expression analyses. DESeq2 was completed using a 2 factor (Genotype + Time + Genotype:Time) model that treated time as a continuous variable, rather than a category (Supplemental Data File 4). An 0.05 p-value and adjusted P-Value (FDR) cutoffs was used to determine significance. PCA was completed with DESeq2 (Love et al., 2014). Comparisons were made at each time point with edgeR with a p-value cutoff of 0.05 and a 1.5 fold change cutoff for significance (Supplemental Data File 4) (Mark D. Robinson, Davis J. McCarthy, 2009). A simple T-test based approach was written in R that used a 0.05 p-value and 2-fold change cutoff (Supplemental Data File 4) and used to compare WT and *atx* TMs at each time point. For all three approaches, WT was compared with TM1 and TM2 separately. The overlap between the TM1 vs WT and TM2 vs WT DEG lists was determined for each statistical method separately using R. The intersection of these DEG lists between the three methods was then identified using http://www.interactivenn.net/. Heatmaps were generated using heatmap.2.

GRN Construction

A script was written in Xcode to be run on a Macbook to analyze DAP-seq data in the NARROWPEAK format (DAPSEQ.sh). Chromosome sequences were provided in the same working directory and BLASTn was run in the terminal. The list of BAGs was overlapped with the total list of transcription factors in *Arabidopsis thaliana*. http://planttfdb.cbi.pku.edu.cn/index.php?sp=Ath. These bolting associated TFs were then overlapped with the mmc2 file provided with the Ecker *et al.* DAP-seq data set to determine which TFs were present. (GEO Dataset GSE60141). The col samples were used for each of the 21 TFs for which binding data were available. R was used to find the intersection between the

lists of TF binding targets and the BAGs. The resulting data were uploaded to cytoscape for visualization.

Accession Numbers
RNA-seq data from this study was made publicly available on GEO as GSE134177.

Supplemental Data Files:
Supplemental Data File 1. T-DNA insertions disrupt gene expression in all three *atx* mutant alleles.

Supplemental Data File 2. *atx* TM phenotype data: All three replicates of raw triple mutant phenotype data are shown along with appropriate statistics and the primers used in this study.

Supplemental Data File 3. Raw FPKM data from the TM RNA-seq Experiment

Supplemental Data File 4. Differential Expression Analysis Code: Annotated code intended for R (Version 1.2.5033) is included for all three DE analyses.

Supplemental Data File 5. Gene Lists

Supplemental Data File 6. BAG expression profiles

Supplemental Data File 7. Reformat.sh: This script was written for a Mac terminal and it takes JSON output files from the Panther Gene Ontology tool and reformats it to make it able to be intersected with time data and used as input in the dcast command in R.

Supplemental Data File 8. DAP-seq.sh: This script takes DAP-seq data in the Narrowpeak format and generates gene names associated with the input genomic locations. It is specific for Arabidopsis and the chromosome sequencences must be present in the same working directory as the program. One must also be able to run BlastN in the terminal. This can be modified to work for ChIP-seq data.

Supplemental Data File 9. DAP-seq binding data for BAG TFs. These data were obtained using the DAP-seq program and include gene accession numbers and associated primary gene symbols generated using the bulk data retrieval tool in TAIR.

Supplemental Data File 10. GRN input file with annotations

Figure Legends

Figure 1: *atx1 atx3 atx4* Triple Mutant (TM) Phenotypes
A: A plant was considered to have bolted when the inflorescence extended 1 centimeter from the base of the rosette. B and C: Real-Time qPCR was used to measure the transcript abundance of two genetic LS markers, *NIT2* and *WRKY75,* in RNA isolated from leaf 6 at day 33. Individual data points shown are the averages of three technical replicates, generated from 6 plants. D: A leaf disc obtained by hole punching leaf 3 harvested at 33 days of age. For statistics, one-way

ANOVAs were run. Then, T-tests with Bonferonni corrected p-values were completed to determine significance. For all data, one representative replicate of three is shown. Results were similar in all three replicates, which can be found in Supplemental Data File 2_Sheets 1-4. Error bars display 95% confidence intervals.

Figure 2: RNA-seq Time Series Experimental Design

WT, *atx* Triple Mutant 1 (TM1), and *atx* Triple Mutant 2 (TM2) were grown in long-day conditions. (n=54 per genotype). Bolting age was scored and plants recorded at the peak of TM bolting (days 24 and 25) were grouped. 10 plants were randomly selected from this group four times in two day increments to ensure that plants were developmentally similar. Leaf 6 was harvested from the 10 plants and stored at -80°C. The 10 leaves were homogenized in liquid nitrogen with a mortar and pestle and then separated into three tubes, which were treated as three replicates/libraries. All harvesting was completed between 8:00 and 10:00 AM to prevent interference by diurnal gene expression changes.

Figure 3: Transcriptome Comparisons

Hierarchical clustering was used to generate a heatmap of transcriptomes, which were generated by averaging expression levels of the three replicates per line at each time point. (T1= *atx* TM1, T2 = *atx* TM2). PCA was completed using the DeSeq2 package for WT vs. TM1 (top) and WT vs. TM2 (bottom) and the resulting charts were manually labeled by genotype and time.

Figure 4: Differential Expression Analysis and Validation

A: DEGs lists from our T-test method (1200), DESeq2 (1536), and edgeR (1978) were overlapped. DEGs identified by at least two of the three statistical methods (750) were considered for validation. B: In order to be considered bolting associated, a gene needed to be differentially expressed in our *atx* triple mutant analysis and at least one of the publicly available WT time-series experiments. Highlighted portions in the Venn diagram mark those selected and used for validation from our analysis, or which genes were considered to be BAGs after validation. Supplemental Data File 5 contains gene lists.

Figure 5: Examples of BAG Expression Across Experiments

Raw data from each experiment were used to generate these graphs in GraphPad PRISM. Data from the *atx* TM and Gaudin *et al.* experiments represent FPKM from RNA-seq, while Breeze *et al.* is Lowess normalized averaged (4 reps) signals in log space from a microarray experiment. Bolting occurs at T0 in the *atx* TM experiment and at Day 21 in the Breeze *et al.* experiment. T0 in the Gaudin *et al.* experiment represents the time of photoperiodic transition from short day to long day conditions. Samples from plants undergoing the vegetative-reproductive transition are shown in black while vegetative control plants are shown in blue.

Figure 6: Bolting Associated Genes (BAGs)

A: Enriched GO terms from a Panther Gene Ontology analysis are shown. B. An ANOVA run on the time-intersected enriched BAGs generated a significant P-value (1.3E-05). Pairwise T-tests were then completed using a Bonferonni corrected p-value (0.05/6 = 0.0083), which indicated that T2 was significantly different than all other time points [p= 0.0003 (T0), 0.0002 (T4), 0.0008 (T6)]. No other significant results were detected. Error bars show the 95 percent confidence intervals. C: A heatmap showing BAG expression levels in all 12 transcriptomes. D.

Short Time Series Expression Miner (STEM) was used to find significant clusters of gene expression changes.

Figure 7: Potential Novel LS Regulators
The Venn Diagram shows overlap between the 398 BAGs, the 2906 DEGs from the DILS dataset, and the 3844 SAGs in the Leaf Senescence Database (LSD). The 91 BAGs that were differentially expressed in the DILS dataset but not in the LSD are highlighted. Select signaling genes from this list of 91 genes are shown in the table along with their direction of gene expression at bolting and during DILS. Gene Symbols/Descriptions were obtained using the bulk data retrieval tool in TAIR.

Figure 8: Bolting Time-Associated Gene Regulatory Network
The network was manually constructed as described in the Methods, and uploaded to Cytoscape for visualization. White nodes were not present in the LSD. Grey nodes were present, but had an unclear function listed in the LSD. Yellow nodes promote LS while green nodes prevent LS. Upregulation is shown by red edges and downregulation is shown with blue edges. Node shape refers to the type of evidence used to determine LS association in LSD 3.0; diamonds represent genomic (microarray) data, triangles represent mutant studies, and squares represent molecular data.

Figure 9: *ERF054* Subnetwork
White nodes were not present in the LSD. Grey nodes were present, but had an unclear function. Yellow nodes promote LS while green nodes prevent LS. Upregulation is shown by red edges and downregulation is shown with blue edges. Node shape refers to the type of evidence used to determine LS association; diamonds represent genomic data, triangles represent mutant studies, and squares represent molecular data. Red labels refer to genes that are differentially expressed during DILS and black labels refer to genes not differentially expressed during DILS. Potential novel LS regulators are shown as white nodes with red labels.

Figure 10: Select Subnetworks
The network was manually constructed in R (description in methods), then uploaded to Cytoscape for visualization. White nodes were not present in the LSD. Grey nodes were present, but had an unclear function. Yellow nodes promote LS while green nodes prevent LS. Upregulation is shown by red edges and downregulation is shown with blue edges. Node shape refers to the type of evidence used to determine LS association; diamonds represent genomic data, triangles represent mutant studies, and squares represent molecular data.

References:
Angeles-Núñez, J. G., & Tiessen, A. (2010). Arabidopsis sucrose synthase 2 and 3 modulate metabolic homeostasis and direct carbon towards starch synthesis in developing seeds. *Planta*, *232*(3), 701–718. https://doi.org/10.1007/s00425-010-1207-9

Asad, M. A. U., Zakari, S. A., Zhao, Q., Zhou, L., Ye, Y., & Cheng, F. (2019). Abiotic stresses intervene with aba signaling to induce destructive metabolic pathways leading to death: Premature leaf senescence in plants. In *International Journal of Molecular Sciences* (Vol. 20, Issue 2). MDPI AG. https://doi.org/10.3390/ijms20020256

Bakshi, M., & Oelmüller, R. (2014). Wrky transcription factors jack of many trades in plants. *Plant Signaling and Behavior, 9*(FEB). https://doi.org/10.4161/psb.27700

Balazadeh, S., Parlitz, S., Mueller-Roeber, B., & Meyer, R. C. (2008). Natural developmental variations in leaf and plant senescence in *Arabidopsis thaliana. Plant Biology, 10*(SUPPL. 1), 136–147. https://doi.org/10.1111/j.1438-8677.2008.00108.x

Bartlett, A., O'Malley, R. C., Huang, S. S. C., Galli, M., Nery, J. R., Gallavotti, A., & Ecker, J. R. (2017). Mapping genome-wide transcription-factor binding sites using DAP-seq. *Nature Protocols, 12*(8), 1659–1672. https://doi.org/10.1038/nprot.2017.055

Berr, A., Shafiq, S., Pinon, V., Dong, A., & Shen, W. H. (2015). The trxG family histone methyltransferase SET DOMAIN GROUP 26 promotes flowering via a distinctive genetic pathway. *Plant Journal, 81*(2), 316–328. https://doi.org/10.1111/tpj.12729

Breeze, E., Harrison, E., McHattie, S., Hughes, L., Hickman, R., Hill, C., Kiddle, S., Kim, Y. S., Penfold, C. A., Jenkins, D., Zhang, C., Morris, K., Jenner, C., Jackson, S., Thomas, B., Tabrett, A., Legaie, R., Moore, J. D., Wild, D. L., … Buchanan-Wollaston, V. (2011). High-resolution temporal profiling of transcripts during Arabidopsis leaf senescence reveals a distinct chronology of processes and regulation. *Plant Cell, 23*(3), 873–894. https://doi.org/10.1105/tpc.111.083345

Brusslan, J. A., Bonora, G., Rus-Canterbury, A. M., Tariq, F., Jaroszewicz, A., & Pellegrini, M. (2015). A genome-wide chronological study of gene expression and two histone modifications, H3K4me3 and H3K9ac, during developmental leaf senescence. *Plant Physiology, 168*(4), 1246–1261. https://doi.org/10.1104/pp.114.252999

Brusslan, J. A., Rus Alvarez-Canterbury, A. M., Nair, N. U., Rice, J. C., Hitchler, M. J., & Pellegrini, M. (2012). Genome-wide evaluation of histone methylation changes associated with leaf senescence in Arabidopsis. *PLoS ONE, 7*(3). https://doi.org/10.1371/journal.pone.0033151

Chen, H. C., Hsieh-Feng, V., Liao, P. C., Cheng, W. H., Liu, L. Y., Yang, Y. W., Lai, M. H., & Chang, M. C. (2017). The function of OsbHLH068 is partially redundant with its homolog, AtbHLH112, in the regulation of the salt stress response but has opposite functions to control flowering in Arabidopsis. *Plant Molecular Biology, 94*(4–5), 531–548. https://doi.org/10.1007/s11103-017-0624-6

Chen, H., Hsieh, E., Cheng, M., Chen, C., Hwang, S., & Lin, T. (2016). ORA47 (octadecanoid-responsive AP2/ERF-domain transcription factor 47) regulates jasmonic acid and abscisic acid biosynthesis and signaling through binding to a novel *cis* -element. *New Phytologist, 211*(2), 599–613. https://doi.org/10.1111/nph.13914

Chen, J., Zhu, X., Ren, J., Qiu, K., Li, Z., Xie, Z., Gao, J., Zhou, X., & Kuai, B. (2017). Suppressor of overexpression of CO 1 negatively regulates dark-induced leaf degreening and senescence by directly repressing pheophytinase and other senescence-associated genes in arabidopsis. *Plant Physiology, 173*(3), 1881–1891. https://doi.org/10.1104/pp.16.01457

Chen, L. Q., Luo, J. H., Cui, Z. H., Xue, M., Wang, L., Zhang, X. Y., Pawlowski, W. P., & He, Y. (2017). ATX3, ATX4, and ATX5 encode putative H3K4 methyltransferases and are critical for plant development. *Plant Physiology, 174*(3), 1795–1806. https://doi.org/10.1104/pp.16.01944

Chen, L., Xiang, S., Chen, Y., Li, D., & Yu, D. (2017). Arabidopsis WRKY45 Interacts with the DELLA Protein RGL1 to Positively Regulate Age-Triggered Leaf Senescence. *Molecular Plant, 10*(9), 1174–1189. https://doi.org/10.1016/j.molp.2017.07.008

Chen, X., Lu, L., Mayer, K. S., Scalf, M., Qian, S., Lomax, A., Smith, L. M., & Zhong, X. (2016). POWERDRESS interacts with HISTONE DEACETYLASE 9 to promote aging in Arabidopsis. *ELife*, *5*(NOVEMBER2016). https://doi.org/10.7554/eLife.17214

Del Prete, S., Molitor, A., Charif, D., Bessoltane, N., Soubigou-Taconnat, L., Guichard, C., Brunaud, V., Granier, F., Fransz, P., & Gaudin, V. (2019). Extensive nuclear reprogramming and endoreduplication in mature leaf during floral induction. *BMC Plant Biology*, *19*(1). https://doi.org/10.1186/s12870-019-1738-6

Deng-Hui, X., Zi-Bing, L., Zu-Yu, Z., K.M., V., Bao-Fang, F., & Zhi-Xiang, C. (2008). *Stress- and Pathogen-Induced Arabidopsis WRKY48 is a Transcriptional Activator that Represses Plant Basal Defense: Molecular Plant*. Molecular Plant. https://www.cell.com/molecular-plant/fulltext/S1674-2052(14)60341-5?_returnURL=https%3A%2F%2Flinkinghub.elsevier.com%2Fretrieve%2Fpii%2FS1674205214603415%3Fshowall%3Dtrue

Dhar, N., Caruana, J., Erdem, I., Subbarao, K. V., Klosterman, S. J., & Raina, R. (2020). The Arabidopsis SENESCENCE-ASSOCIATED GENE 13 Regulates Dark-Induced Senescence and Plays Contrasting Roles in Defense Against Bacterial and Fungal Pathogens . *Molecular Plant-Microbe Interactions®*, MPMI-11-19-0329. https://doi.org/10.1094/mpmi-11-19-0329-r

Ernst, J., & Bar-Joseph, Z. (2006). STEM: A tool for the analysis of short time series gene expression data. *BMC Bioinformatics*, *7*(1), 191. https://doi.org/10.1186/1471-2105-7-191

Fernández-Calvino, L., Guzmán-Benito, I., del Toro, F. J., Donaire, L., Castro-Sanz, A. B., Ruíz-Ferrer, V., & Llave, C. (2016). Activation of senescence-associated Dark-inducible (DIN) genes during infection contributes to enhanced susceptibility to plant viruses. *Molecular Plant Pathology*, *17*(1), 3–15. https://doi.org/10.1111/mpp.12257

Gachomo, E. W., Jno Baptiste, L., Kefela, T., Saidel, W. M., & Kotchoni, S. O. (2014). The Arabidopsis CURVY1 (CVY1) gene encoding a novel receptor-like protein kinase regulates cell morphogenesis, flowering time and seed production. *BMC Plant Biology*, *14*(1), 221. https://doi.org/10.1186/s12870-014-0221-7

Gibalová, A., Reňák, D., Matczuk, K., Dupl'Áková, N., Cháb, D., Twell, D., & Honys, D. (2009). AtbZIP34 is required for Arabidopsis pollen wall patterning and the control of several metabolic pathways in developing pollen. *Plant Molecular Biology*, *70*(5), 581–601. https://doi.org/10.1007/s11103-009-9493-y

Guo, P., Li, Z., Huang, P., Li, B., Fang, S., Chu, J., & Guo, H. (2017). A tripartite amplification loop involving the transcription factor WRKY75, salicylic acid, and reactive oxygen species accelerates leaf senescence. *Plant Cell*, *29*(11), 2854–2870. https://doi.org/10.1105/tpc.17.00438

Havé, M., Marmagne, A., Chardon, F., & Masclaux-Daubresse, C. (2017). Nitrogen remobilization during leaf senescence: lessons from Arabidopsis to crops. *Journal of Experimental Botany*, *68*(10), 2513–2529. https://doi.org/10.1093/jxb/erw365

Hensel, L. L., Grbić, V., Baumgarten, D. A., & Bleecker, A. B. (1993). Developmental and age-related processes that influence the longevity and senescence of photosynthetic tissues in arabidopsis. *The Plant Cell*, *5*(5), 553–564. https://doi.org/10.1105/tpc.5.5.553

Hinckley, W. E., Keymanesh, K., Cordova, J. A., & Brusslan, J. A. (2019). The HAC1 histone acetyltransferase promotes leaf senescence and regulates the expression of ERF022. *Plant Direct*, *3*(8). https://doi.org/10.1002/pld3.159

Huaiyu Mi, Anushya Muruganujan, P. D. T. (2012). *PANTHER in 2013: modeling the evolution of gene function, and other gene attributes, in the context of phylogenetic trees | Nucleic Acids Research | Oxford Academic*. Nucleic Acids Research. https://academic.oup.com/nar/article/41/D1/D377/1060482

Jeongsik Kim, Su Jin Park, Il Hwan Lee, Hyosub Chu, Christopher A Penfold, Jin Hee Kim, Vicky Buchanan-Wollaston, Hong Gil Nam, Hye Ryun Woo, P. O. L. (2018). *Comparative transcriptome analysis in Arabidopsis ein2/ore3 and ahk3/ore12 mutants during dark-induced leaf senescence | Journal of Experimental Botany | Oxford Academic*. Journal of Experimental Botany. https://academic.oup.com/jxb/article/69/12/3023/4965898

Jiang, J., Ma, S., Ye, N., Jiang, M., Cao, J., & Zhang, J. (2017). WRKY transcription factors in plant responses to stresses. In *Journal of Integrative Plant Biology* (Vol. 59, Issue 2, pp. 86–101). Blackwell Publishing Ltd. https://doi.org/10.1111/jipb.12513

Jing, H. C., Schippers, J. H. M., Hille, J., & Dijkwel, P. P. (2005). Ethylene-induced leaf senescence depends on age-related changes and OLD genes in Arabidopsis. *Journal of Experimental Botany*, *56*(421), 2915–2923. https://doi.org/10.1093/jxb/eri287

Joël Simoneau, Simon Dumontier, Ryan Gosselin, M. S. S. (2019). *Current RNA-seq methodology reporting limits reproducibility | Briefings in Bioinformatics | Oxford Academic*. Briefings in Bioinformatics. https://academic.oup.com/bib/advance-article/doi/10.1093/bib/bbz124/5669860

Katari, M. S., Nowicki, S. D., Aceituno, F. F., Nero, D., Kelfer, J., Thompson, L. P., Cabello, J. M., Davidson, R. S., Goldberg, A. P., Shasha, D. E., Coruzzi, G. M., & Gutiérrez, R. A. (2010). VirtualPlant: A software platform to support systems biology research. *Plant Physiology*, *152*(2), 500–515. https://doi.org/10.1104/pp.109.147025

Keqiang Wu, Lin Zhang, Changhe Zhou, Chun-Wei Yu, V. C. (2008). *HDA6 is required for jasmonate response, senescence and flowering in Arabidopsis | Journal of Experimental Botany | Oxford Academic*. Journal of Experimental Botany. https://academic.oup.com/jxb/article/59/2/225/536848

Khanna-Chopra, R. (2012). Leaf senescence and abiotic stresses share reactive oxygen species-mediated chloroplast degradation. In *Protoplasma* (Vol. 249, Issue 3, pp. 469–481). https://doi.org/10.1007/s00709-011-0308-z

Kim, H. J., Chiang, Y. H., Kieber, J. J., & Schaller, G. E. (2013). SCFKMD controls cytokinin signaling by regulating the degradation of type-B response regulators. *Proceedings of the National Academy of Sciences of the United States of America*, *110*(24), 10028–10033. https://doi.org/10.1073/pnas.1300403110

Kim, H. J., Nam, H. G., & Lim, P. O. (2016). Regulatory network of NAC transcription factors in leaf senescence. In *Current Opinion in Plant Biology* (Vol. 33, pp. 48–56). Elsevier Ltd. https://doi.org/10.1016/j.pbi.2016.06.002

Kim, H. J., Park, J. H., Kim, J., Kim, J. J., Hong, S., Kim, J., Kim, J. H., Woo, H. R., Hyeon, C., Lim, P. O., Nam, H. G., & Hwang, D. (2018). Time-evolving genetic networks reveal a nac troika that negatively regulates leaf senescence in arabidopsis. *Proceedings of the National Academy of Sciences of the United States of America*, *115*(21), E4930–E4939. https://doi.org/10.1073/pnas.1721523115

Kim, T., Kang, K., Kim, S. H., An, G., & Paek, N. C. (2019). OsWRKY5 promotes rice leaf senescence via senescence-associated NAC and abscisic acid biosynthesis pathway. *International Journal of Molecular Sciences*, *20*(18). https://doi.org/10.3390/ijms20184437

Kiyotoshi Takeno. (2016). *Stress-induced flowering: the third category of flowering response. - PubMed - NCBI*. Journal of Experimental Botany. https://www.ncbi.nlm.nih.gov/pubmed/27382113

Koyama, T. (2014). The roles of ethylene and transcription factors in the regulation of onset of leaf senescence. In *Frontiers in Plant Science* (Vol. 5, Issue NOV). Frontiers Media S.A. https://doi.org/10.3389/fpls.2014.00650

Koyama, T., Nii, H., Mitsuda, N., Ohta, M., Kitajima, S., Ohme-Takagi, M., & Sato, F. (2013). A regulatory cascade involving class II ETHYLENE RESPONSE FACTOR transcriptional repressors operates in the progression of leaf senescence. *Plant Physiology*, *162*(2), 991–1005. https://doi.org/10.1104/pp.113.218115

Lei, W., Li, Y., Yao, X., Qiao, K., Wei, L., Liu, B., Zhang, D., & Lin, H. (2020). NAP is involved in GA-mediated chlorophyll degradation and leaf senescence by interacting with DELLAs in Arabidopsis. *Plant Cell Reports*, *39*(1), 75–87. https://doi.org/10.1007/s00299-019-02474-2

Li, W., Li, X., Chao, J., Zhang, Z., Wang, W., & Guo, Y. (2018). NAC family transcription factors in tobacco and their potential role in regulating leaf senescence. *Frontiers in Plant Science*, *871*. https://doi.org/10.3389/fpls.2018.01900

Liu, P., Zhang, S., Zhou, B., Luo, X., Zhou, X. F., Cai, B., Jin, Y. H., Niu, D., Lin, J., Cao, X., & Jin, J. B. (2019). The histone H3K4 demethylase JMJ16 represses leaf senescence in arabidopsis. *Plant Cell*, *31*(2), 430–443. https://doi.org/10.1105/tpc.18.00693

Liu, Y., Ji, X., Nie, X., Qu, M., Zheng, L., Tan, Z., Zhao, H., Huo, L., Liu, S., Zhang, B., & Wang, Y. (2015). *Arabidopsis* AtbHLH112 regulates the expression of genes involved in abiotic stress tolerance by binding to their E-box and GCG-box motifs. *New Phytologist*, *207*(3), 692–709. https://doi.org/10.1111/nph.13387

Love, M. I., Huber, W., & Anders, S. (2014). Moderated estimation of fold change and dispersion for RNA-seq data with DESeq2. *Genome Biology*, *15*(12). https://doi.org/10.1186/s13059-014-0550-8

Lu, Y., Truman, W., Liu, X., Bethke, G., Zhou, M., Myers, C. L., Katagiri, F., & Glazebrook, J. (2018). Different modes of negative regulation of plant immunity by calmodulin-related genes. *Plant Physiology*, *176*(4), 3046–3061. https://doi.org/10.1104/pp.17.01209

Luquez VM, Sasal Y, Medrano M, Martín MI, Mujica M, G. J. (2006). *Quantitative trait loci analysis of leaf and plant longevity in Arabidopsis thaliana. - PubMed - NCBI*. Journal of Experimental Botany. https://www.ncbi.nlm.nih.gov/pubmed/16547126

Mahmood, K., El-Kereamy, A., Kim, S.-H., Nambara, E., & Rothstein, S. J. (2016). ANAC032 Positively Regulates Age-Dependent and Stress-Induced Senescence in Arabidopsis thaliana. *Plant and Cell Physiology*, *57*(10), 2029–2046. https://doi.org/10.1093/pcp/pcw120

Marian Bemer, Hilda van Mourik, Jose M Muiño, Cristina Ferrándiz, Kerstin Kaufmann, G. C. A. (2017). *FRUITFULL controls SAUR10 expression and regulates Arabidopsis growth and architecture | Journal of Experimental Botany | Oxford Academic*. Journal of Experimental Botany. https://academic.oup.com/jxb/article/68/13/3391/3861879

Mark D. Robinson, Davis J. McCarthy, G. K. S. (2009). *edgeR: a Bioconductor package for differential expression analysis of digital gene expression data | Bioinformatics | Oxford Academic.* Bioinformatics. https://academic.oup.com/bioinformatics/article/26/1/139/182458

Miao, Y., Laun, T., Zimmermann, P., & Zentgraf, U. (2004). Targets of the WRKY53 transcription factor and its role during leaf senescence in Arabidopsis. *Plant Molecular Biology*, *55*(6), 853–867. https://doi.org/10.1007/s11103-004-2142-6

Mouradov, A., Cremer, F., & Coupland, G. (2002). Control of flowering time: Interacting pathways as a basis for diversity. *Plant Cell*, *14*(SUPPL.), s111. https://doi.org/10.1105/tpc.001362

Müller, B., Fastner, A., Karmann, J., Mansch, V., Hoffmann, T., Schwab, W., Suter-Grotemeyer, M., Rentsch, D., Truernit, E., Ladwig, F., Bleckmann, A., Dresselhaus, T., & Hammes, U. Z. (2015). Amino acid export in developing arabidopsis seeds depends on UmamiT facilitators. *Current Biology*, *25*(23), 3126–3131. https://doi.org/10.1016/j.cub.2015.10.038

Nguyen, K. T., Park, J., Park, E., Lee, I., & Choi, G. (2015). The Arabidopsis RING Domain Protein BOI Inhibits Flowering via CO-dependent and CO-independent Mechanisms. *Molecular Plant*, *8*(12), 1725–1736. https://doi.org/10.1016/j.molp.2015.08.005

Nicole Ay, Bianka Janack, K. H. (2014). *Epigenetic control of plant senescence and linked processes | Journal of Experimental Botany | Oxford Academic.* Journal of Experimental Botany. https://academic.oup.com/jxb/article/65/14/3875/2877487

Nir Sade, María del Mar Rubio-Wilhelmi, Kamolchanok Umnajkitikorn, E. B. (2018). *Stress-induced senescence and plant tolerance to abiotic stress | Journal of Experimental Botany | Oxford Academic.* Journal of Experimental Botany. https://academic.oup.com/jxb/article/69/4/845/4036238

Nooden, L. D., Guiamet, J. J., & John, I. (1997). Senescence mechanisms. *Physiologia Plantarum*, *101*(4), 746–753. https://doi.org/10.1111/j.1399-3054.1997.tb01059.x

O'Malley, R. C., Huang, S. S. C., Song, L., Lewsey, M. G., Bartlett, A., Nery, J. R., Galli, M., Gallavotti, A., & Ecker, J. R. (2016). Cistrome and Epicistrome Features Shape the Regulatory DNA Landscape. *Cell*, *165*(5), 1280–1292. https://doi.org/10.1016/j.cell.2016.04.038

Oda-Yamamizo, C., Mitsuda, N., Sakamoto, S., Ogawa, D., Ohme-Takagi, M., & Ohmiya, A. (2016). The NAC transcription factor ANAC046 is a positive regulator of chlorophyll degradation and senescence in Arabidopsis leaves. *Scientific Reports*, *6*(1), 1–13. https://doi.org/10.1038/srep23609

Olas, J. J., & Wahl, V. (2019). Tissue-specific NIA1 and NIA2 expression in Arabidopsis thaliana. *Plant Signaling and Behavior*, *14*(11). https://doi.org/10.1080/15592324.2019.1656035

Ougham, H., Hörtensteiner, S., Armstead, I., Donnison, I., King, I., Thomas, H., & Mur, L. (2008). The control of chlorophyll catabolism and the status of yellowing as a biomarker of leaf senescence. *Plant Biology*, *10*(SUPPL. 1), 4–14. https://doi.org/10.1111/j.1438-8677.2008.00081.x

Pelaz, S., Ditta, G. S., Baumann, E., Wisman, E., & Yanofsky, M. F. (2000). B and C floral organ identity functions require SEPALLATTA MADS-box genes. *Nature*, *405*(6783), 200–203. https://doi.org/10.1038/35012103

Pien, S., Fleury, D., Mylne, J. S., Crevillen, P., Inzé, D., Avramova, Z., Dean, C., & Grossniklaus, U. (2008). Arabidopsis Trithorax1 dynamically regulates Flowering Locus C activation via histone 3 lysine 4 trimethylation. *Plant Cell*, *20*(3), 580–588. https://doi.org/10.1105/tpc.108.058172

Pontvianne, F., Blevins, T., & Pikaard, C. S. (2010). Arabidopsis Histone Lysine Methyltransferases. In *Advances in Botanical Research* (Vol. 53, pp. 1–22). Academic Press. https://doi.org/10.1016/s0065-2296(10)53001-5

Porra, R. J., Thompson, W. A., & Kriedemann, P. E. (1989). Determination of accurate extinction coefficients and simultaneous equations for assaying chlorophylls a and b extracted with four different solvents: verification of the concentration of chlorophyll standards by atomic absorption spectroscopy. *BBA - Bioenergetics*, *975*(3), 384–394. https://doi.org/10.1016/S0005-2728(89)80347-0

Qiu, K., Li, Z., Yang, Z., Chen, J., Wu, S., Zhu, X., Gao, S., Gao, J., Ren, G., Kuai, B., & Zhou, X. (2015). EIN3 and ORE1 Accelerate Degreening during Ethylene-Mediated Leaf Senescence by Directly Activating Chlorophyll Catabolic Genes in Arabidopsis. *PLoS Genetics*, *11*(7). https://doi.org/10.1371/journal.pgen.1005399

Raines, T., Shanks, C., Cheng, C. Y., McPherson, D., Argueso, C. T., Kim, H. J., Franco-Zorrilla, J. M., Lõpez-Vidriero, I., Solano, R., Vaňková, R., Schaller, G. E., & Kieber, J. J. (2016). The cytokinin response factors modulate root and shoot growth and promote leaf senescence in Arabidopsis. *Plant Journal*, *85*(1), 134–147. https://doi.org/10.1111/tpj.13097

Riefler, M., Novak, O., Strnad, M., & Schmülling, T. (2006). Arabidopsis cytokinin receptors mutants reveal functions in shoot growth, leaf senescence, seed size, germination, root development, and cytokinin metabolism. *Plant Cell*, *18*(1), 40–54. https://doi.org/10.1105/tpc.105.037796

Ryu, J. Y., Park, C. M., & Seo, P. J. (2011). The floral repressor BROTHER OF FT AND TFL1 (BFT) modulates flowering initiation under High salinity in Arabidopsis. *Molecules and Cells*, *32*(3), 295–303. https://doi.org/10.1007/s10059-011-0112-9

Schenk, P. M., Kazan, K., Rusu, A. G., Manners, J. M., & Maclean, D. J. (2005). The SEN1 gene of Arabidopsis is regulated by signals that link plant defence responses and senescence. *Plant Physiology and Biochemistry*, *43*(10–11), 997–1005. https://doi.org/10.1016/j.plaphy.2005.09.002

Shannon, P., Markiel, A., Ozier, O., Baliga, N. S., Wang, J. T., Ramage, D., Amin, N., Schwikowski, B., & Ideker, T. (2003). Cytoscape: A software Environment for integrated models of biomolecular interaction networks. *Genome Research*, *13*(11), 2498–2504. https://doi.org/10.1101/gr.1239303

Song, Y. H., Kubota, A., Kwon, M. S., Covington, M. F., Lee, N., Taagen, E. R., Laboy Cintrón, D., Hwang, D. Y., Akiyama, R., Hodge, S. K., Huang, H., Nguyen, N. H., Nusinow, D. A., Millar, A. J., Shimizu, K. K., & Imaizumi, T. (2018). Molecular basis of flowering under natural long-day conditions in Arabidopsis. *Nature Plants*, *4*(10), 824–835. https://doi.org/10.1038/s41477-018-0253-3

Tamada, Y., Yun, J. Y., Woo, S. C., & Amasino, R. M. (2009). ARABIDOPSIS TRITHORAX-RELATED7 is required for methylation of lysine 4 of histone H3 and for transcriptional activation of FLOWERING LOCUS C. *Plant Cell*, *21*(10), 3257–3269. https://doi.org/10.1105/tpc.109.070060

Tamary, E., Nevo, R., Naveh, L., Levin-Zaidman, S., Kiss, V., Savidor, A., Levin, Y., Eyal, Y., Reich, Z., & Adam, Z. (2019). Chlorophyll catabolism precedes changes in chloroplast structure and proteome during leaf senescence. *Plant Direct*, *3*(3). https://doi.org/10.1002/pld3.127

Thomas, P. D., Campbell, M. J., Kejariwal, A., Mi, H., Karlak, B., Daverman, R., Diemer, K., Muruganujan, A., & Narechania, A. (2003). PANTHER: A library of protein families and

subfamilies indexed by function. *Genome Research*, *13*(9), 2129–2141. https://doi.org/10.1101/gr.772403

Tian, T., Ma, L., Liu, Y., Xu, D., Chen, Q., & Li, G. (2020). Arabidopsis FAR-RED ELONGATED HYPOCOTYL3 Integrates Age and Light Signals to Negatively Regulate Leaf Senescence. *The Plant Cell*, tpc.00021.2020. https://doi.org/10.1105/tpc.20.00021

Townsley, B. T., Covington, M. F., Ichihashi, Y., Zumstein, K., & Sinha, N. R. (2015). BrAD-seq: Breath Adapter Directional sequencing: a streamlined, ultra-simple and fast library preparation protocol for strand specific mRNA library construction. *Frontiers in Plant Science*, *6*(MAY), 1–11. https://doi.org/10.3389/fpls.2015.00366

Tsutsui, T., Kato, W., Asada, Y., Sako, K., Sato, T., Sonoda, Y., Kidokoro, S., Yamaguchi-Shinozaki, K., Tamaoki, M., Arakawa, K., Ichikawa, T., Nakazawa, M., Seki, M., Shinozaki, K., Matsui, M., Ikeda, A., & Yamaguchi, J. (2009). DEAR1, a transcriptional repressor of DREB protein that mediates plant defense and freezing stress responses in Arabidopsis. *Journal of Plant Research*, *122*(6), 633–643. https://doi.org/10.1007/s10265-009-0252-6

van Verk, M. C., Bol, J. F., & Linthorst, H. J. M. (2011). WRKY Transcription Factors Involved in Activation of SA Biosynthesis Genes. *BMC Plant Biology*, *11*(1), 89. https://doi.org/10.1186/1471-2229-11-89

Vicente Balanzà, Irene Martínez-Fernández, C. F. (2014). *Sequential action of FRUITFULL as a modulator of the activity of the floral regulators SVP and SOC1 | Journal of Experimental Botany | Oxford Academic*. Journal of Experimental Botany. https://academic.oup.com/jxb/article/65/4/1193/498956

Wada, K. C., & Takeno, K. (2010). Stress-induced flowering. *Plant Signaling & Behavior*, *5*(8), 944–947. https://doi.org/10.4161/psb.5.8.11826

Wang, X., Gao, J., Gao, S., Song, Y., Yang, Z., & Kuai, B. (2019). The H3K27me3 demethylase REF6 promotes leaf senescence through directly activating major senescence regulatory and functional genes in Arabidopsis. *PLoS Genetics*, *15*(4), e1008068. https://doi.org/10.1371/journal.pgen.1008068

Wang, Z., Qian, C., Guo, X., Liu, E., Mao, K., Mu, C., Chen, N., Zhang, W., & Liu, H. (2016). ELS1, a novel MATE transporter related to leaf senescence and iron homeostasis in Arabidopsis thaliana. *Biochemical and Biophysical Research Communications*, *476*(4), 319–325. https://doi.org/10.1016/j.bbrc.2016.05.121

Weaver, L. M., Gan, S., Quirino, B., & Amasino, R. M. (1998). A comparison of the expression patterns of several senescence-associated genes in response to stress and hormone treatment. *Plant Molecular Biology*, *37*(3), 455–469. https://doi.org/10.1023/A:1005934428906

Wen, Z., Mei, Y., Zhou, J., Cui, Y., Wang, D., & Wang, N. N. (2020). SAUR49 Can Positively Regulate Leaf Senescence by Suppressing SSPP in Arabidopsis. *Plant and Cell Physiology*, *61*(3), 644–658. https://doi.org/10.1093/pcp/pcz231

Wong, M. M., Bhaskara, G. B., Wen, T. N., Lin, W. D., Nguyen, T. T., Chong, G. L., & Verslues, P. E. (2019). Phosphoproteomics of Arabidopsis Highly ABA-Induced1 identifies AT-Hook-Like10 phosphorylation required for stress growth regulation. *Proceedings of the National Academy of Sciences of the United States of America*, *116*(6), 2354–2363. https://doi.org/10.1073/pnas.1819971116

Woo, H. R., Kim, H. J., Lim, P. O., & Nam, H. G. (2019). Leaf Senescence: Systems and Dynamics Aspects. *Annual Review of Plant Biology*, *70*(1), 347–376. https://doi.org/10.1146/annurev-arplant-050718-095859

Woo, H. R., Kim, H. J., Nam, H. G., & Lim, P. O. (2013). Plant leaf senescence and death - regulation by multiple layers of control and implications for aging in general. *Journal of Cell Science*, *126*(21), 4823–4833. https://doi.org/10.1242/jcs.109116

Xiao, D., Cui, Y., Xu, F., Xu, X., Gao, G., Wang, Y., Guo, Z., Wang, D., & Wang, N. N. (2015). SENESCENCE-SUPPRESSED PROTEIN PHOSPHATASE directly interacts with the cytoplasmic domain of SENESCENCE-ASSOCIATED RECEPTOR-LIKE KINASE and negatively regulates leaf senescence in arabidopsis. *Plant Physiology*, *169*(2), 1275–1291. https://doi.org/10.1104/pp.15.01112

Yan, Z., Jia, J., Yan, X., Shi, H., & Han, Y. (2017). Arabidopsis KHZ1 and KHZ2, two novel non-tandem CCCH zinc-finger and K-homolog domain proteins, have redundant roles in the regulation of flowering and senescence. *Plant Molecular Biology*, *95*(6), 549–565. https://doi.org/10.1007/s11103-017-0667-8

Yuehui, H., Hirotada, F., David F., H., & Susheng, G. (2002). Evidence Supporting a Role of Jasmonic Acid in Arabidopsis Leaf Senescence. *Plant Physiology*, *127*(3), 435–441. https://doi.org/10.1104/pp.010843.)

Yun, J.-Y., Tamada, Y., Kang, Y. E., & Amasino, R. M. (n.d.). *ARABIDOPSIS TRITHORAX-RELATED3/SET DOMAIN GROUP2 is Required for the Winter-Annual Habit of Arabidopsis thaliana*. https://doi.org/10.1093/pcp/pcs021

Yun, J.-Y., Tamada, Y., Kang, Y. E., & Amasino, R. M. (2012). ARABIDOPSIS TRITHORAX-RELATED3/SET DOMAIN GROUP2 is Required for the Winter-Annual Habit of Arabidopsis thaliana. *Plant and Cell Physiology*, *53*(5), 834–846. https://doi.org/10.1093/pcp/pcs021

Zentgraf, U., & Doll, J. (2019). Arabidopsis wrky53, a node of multi-layer regulation in the network of senescence. In *Plants* (Vol. 8, Issue 12). MDPI AG. https://doi.org/10.3390/plants8120578

Zhang, H., Zhu, H., Pan, Y., Yu, Y., Luan, S., & Li, L. (2014). *A DTX/MATE-Type Transporter Facilitates Abscisic Acid Efflux and Modulates ABA Sensitivity and Drought Tolerance in Arabidopsis: Molecular Plant*. Molecular Plant. https://www.cell.com/molecular-plant/fulltext/S1674-2052(14)60957-6?_returnURL=https%3A%2F%2Flinkinghub.elsevier.com%2Fretrieve%2Fpii%2FS1674205214609576%3Fshowall%3Dtrue

Zhang, K., & Gan, S. S. (2012). An abscisic acid-AtNAP transcription factor-SAG113 protein phosphatase 2C regulatory chain for controlling dehydration in senescing Arabidopsis leaves. *Plant Physiology*, *158*(2), 961–969. https://doi.org/10.1104/pp.111.190876

Zhang, K., Halitschke, R., Yin, C., Liu, C.-J., & Gan, S.-S. (2013). Salicylic acid 3-hydroxylase regulates Arabidopsis leaf longevity by mediating salicylic acid catabolism. *Proceedings of the National Academy of Sciences of the United States of America*, *110*(36), 14807–14812. https://doi.org/10.1073/pnas.1302702110

Zhang, L., Chen, L., & Yu, D. (2018). Transcription factor WRKY75 interacts with DELLA proteins to affect flowering. *Plant Physiology*, *176*(1), 790–803. https://doi.org/10.1104/pp.17.00657

Zhang, Z., Shi, L., Dawany, N., Kelsen, J., Petri, M. A., & Sullivan, K. E. (2016). H3K4 tri-methylation breadth at transcription start sites impacts the transcriptome of systemic lupus erythematosus. *Clinical Epigenetics*, *8*(1), 14. https://doi.org/10.1186/s13148-016-0179-4

Zhao, Y., Gao, J., Im Kim, J., Chen, K., Bressan, R. A., & Zhu, J.-K. (2017). Control of Plant Water Use by ABA Induction of Senescence and Dormancy: An Overlooked Lesson from Evolution. *Plant & Cell Physiology*, *58*(8), 1319–1327. https://doi.org/10.1093/pcp/pcx086

Zhonghai Li, Yang Zhang, Dong Zou, Yi Zhao, Hou-Ling Wang, Yi Zhang, Xinli Xia, Jingchu Luo, Hongwei Guo, Z. Z. (2019). *LSD 3.0: a comprehensive resource for the leaf senescence research community | Nucleic Acids Research | Oxford Academic*. Nucleic Acids Research. https://academic.oup.com/nar/article/48/D1/D1069/5584839
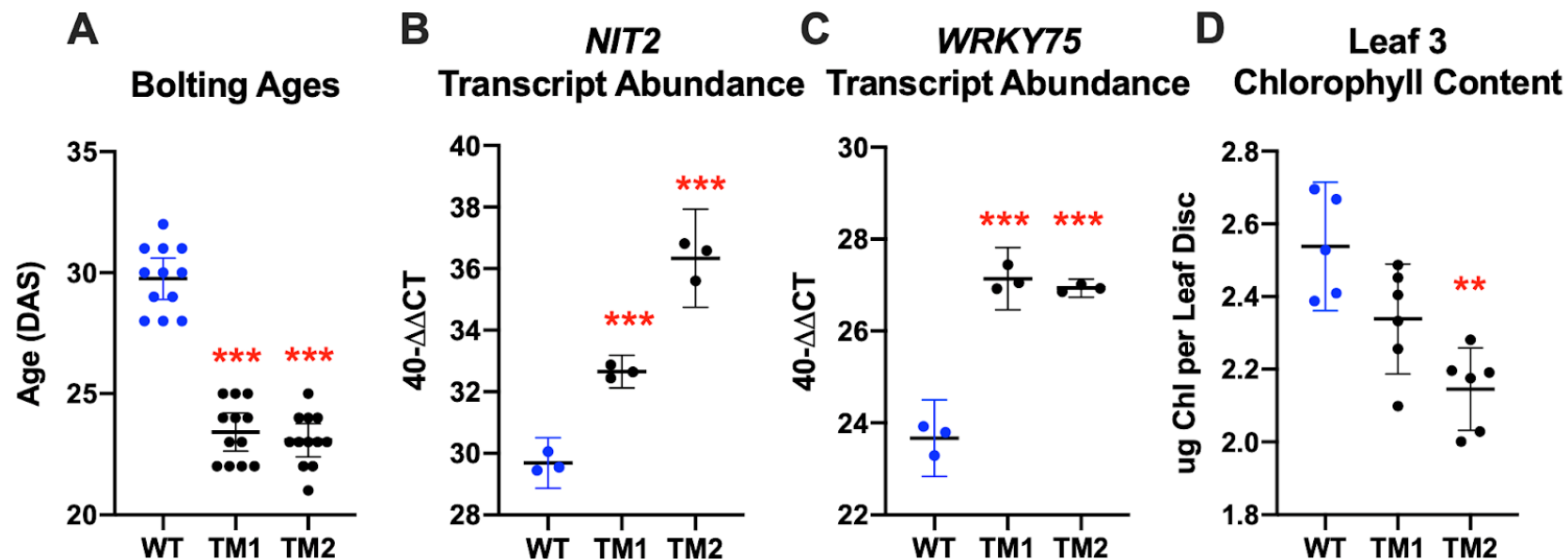
Figure 1: *atx1 atx3 atx4* Triple Mutant (TM) Phenotypes
A: A plant was considered to have bolted when the inflorescence extended 1 centimeter from the base of the rosette. B and C: Real-Time qPCR was used to measure the transcript abundance of two genetic LS markers, *NIT2* and *WRKY75,* in RNA isolated from leaf 6 at day 33. Individual data points shown are the averages of three technical replicates, generated from 6 plants. D: A leaf disc obtained by hole punching leaf 3 at day 33 was suspended in DMF in the dark overnight. The resulting solution was quantified in a quartz plate.. For statistics, one-way ANOVAs were run. Then, both Tukey Kramer Tests and T-tests with Bonferonni corrected p-values were completed to determine significance. Both tests generated largely the same results (Supp fig). For all data, one representative replicate of three is shown. Results were similar in all three replicates, which can be found in supplemental file 1. Error bars display 95 confidence intervals.

Age (DAS)	23	25	27	29	31	33
atx1,atx3,atx4 triple mutant		T0 1 cm [Bolting Plants Pooled	T2	T4	T6	Accelerated leaf senescence phenotype detected in triple mutants relative to WT. (Figure 1)
Number of cDNA libraries: →	All plants watered with nutrients. Leaf 6 labeled with loose thread.	TM1: 3 TM2: 3	TM1: 3 TM2: 3	TM1: 3 TM2: 3	TM1: 3 TM2: 3	
WT (Col 0)					1 cm [	
Number of cDNA libraries: →		WT: 3	WT: 3	WT: 3	WT: 3	

Figure 2: RNA-seq Time Series Experimental Design

WT, *atx* Triple Mutant 1 (TM1), and *atx* Triple Mutant 2 (TM2) were grown in long-day conditions. (n=54 per genotype). Bolting age was scored and plants recorded at the peak of TM bolting (days 24 and 25) were grouped. 10 plants were randomly selected from this group four times in two day increments to ensure that plants were developmentally similar. Leaf 6 was harvested from the 10 plants and stored at -80°C. The 10 leaves were homogenized in liquid nitrogen with a mortar and pestle and then separated into three tubes, which were treated as three replicates/libraries. All harvesting was completed between 8:00 and 10:00 AM to prevent interference by diurnal gene expression changes.
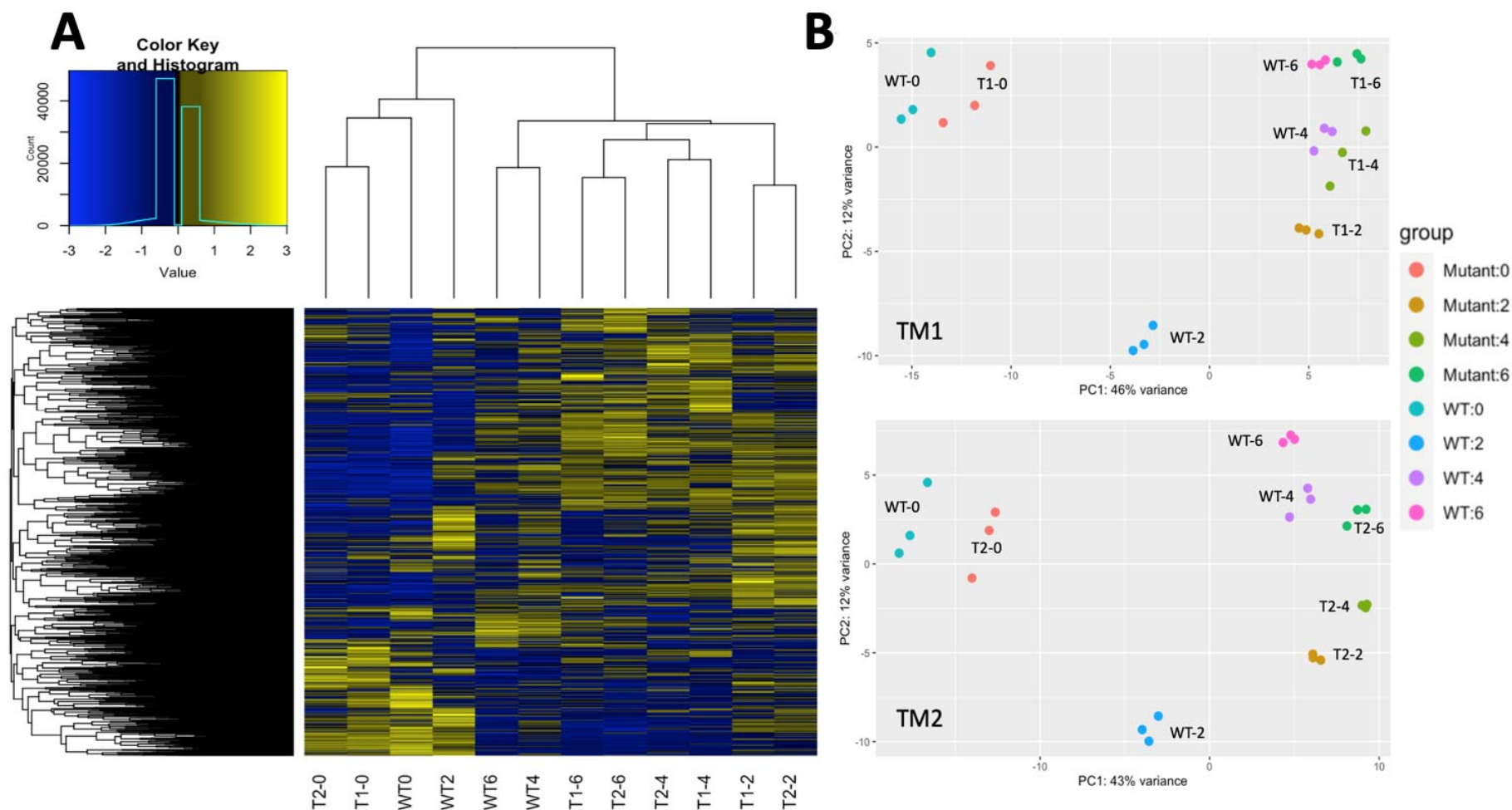
Figure 3: Transcriptome Comparisons

Hierarchical clustering was used to generate a heatmap of transcriptomes, which were generated by averaging expression levels of the three replicates per line at each time point. (T1= *atx* TM1, T2 = *atx* TM2). PCA was completed using the DeSeq2 package and the resulting charts were manually labeled by genotype and time.
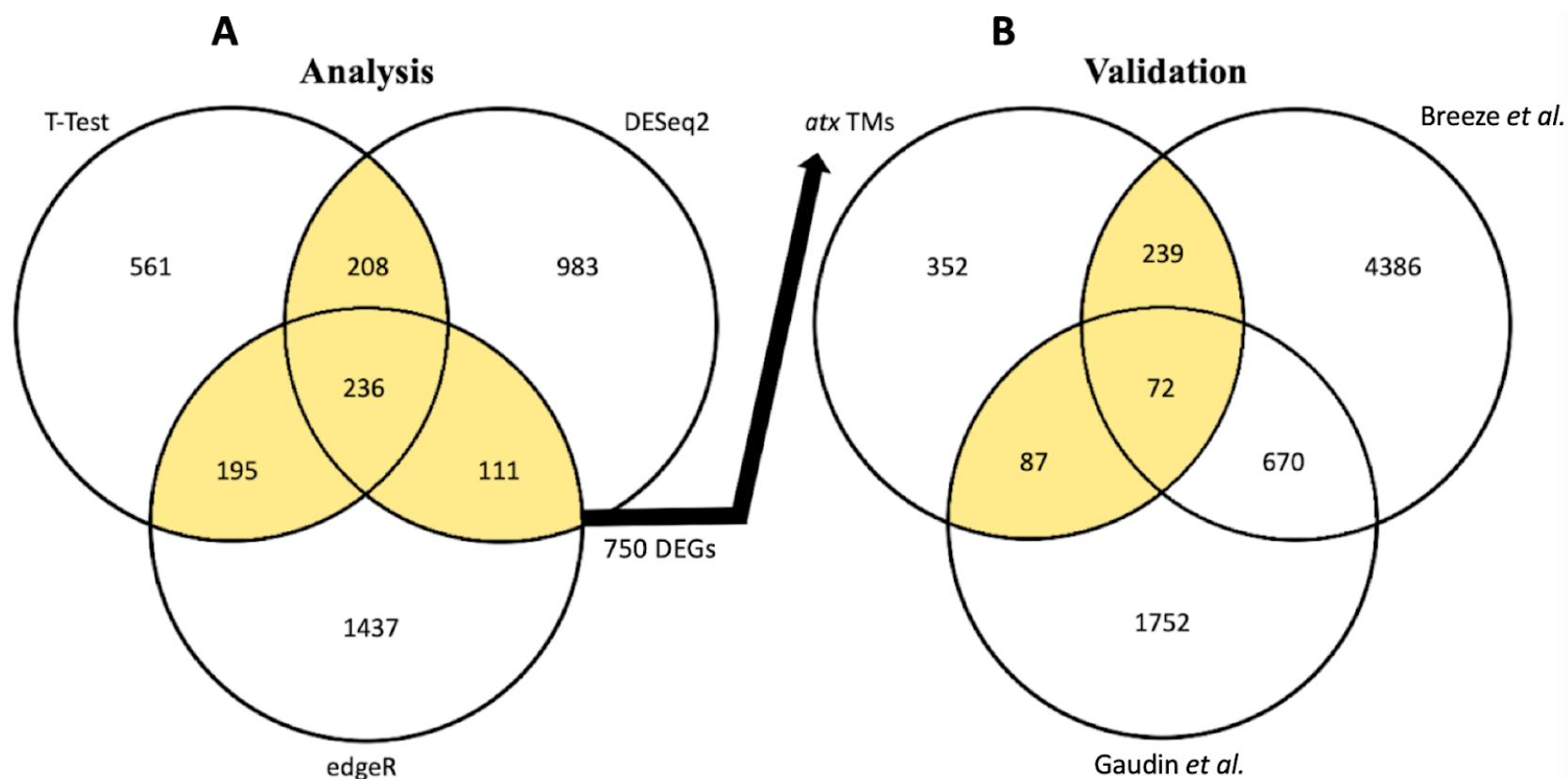
Figure 4: Differential Expression Analysis and Validation
A: DEGs lists from our T-test method (1200), DESeq2 (1536), and edgeR (1978) were overlapped. DEGs identified by at least two of the three statistical methods (750) were considered for validation. B: In order to be considered bolting associated, a gene needed to be differentially expressed in our *atx* triple mutant analysis and at least one of the publicly available WT time-series experiments. Highlighted portions in the Venn diagram mark those selected and used for validation from our analysis, or which genes were considered to be BAGs after validation.
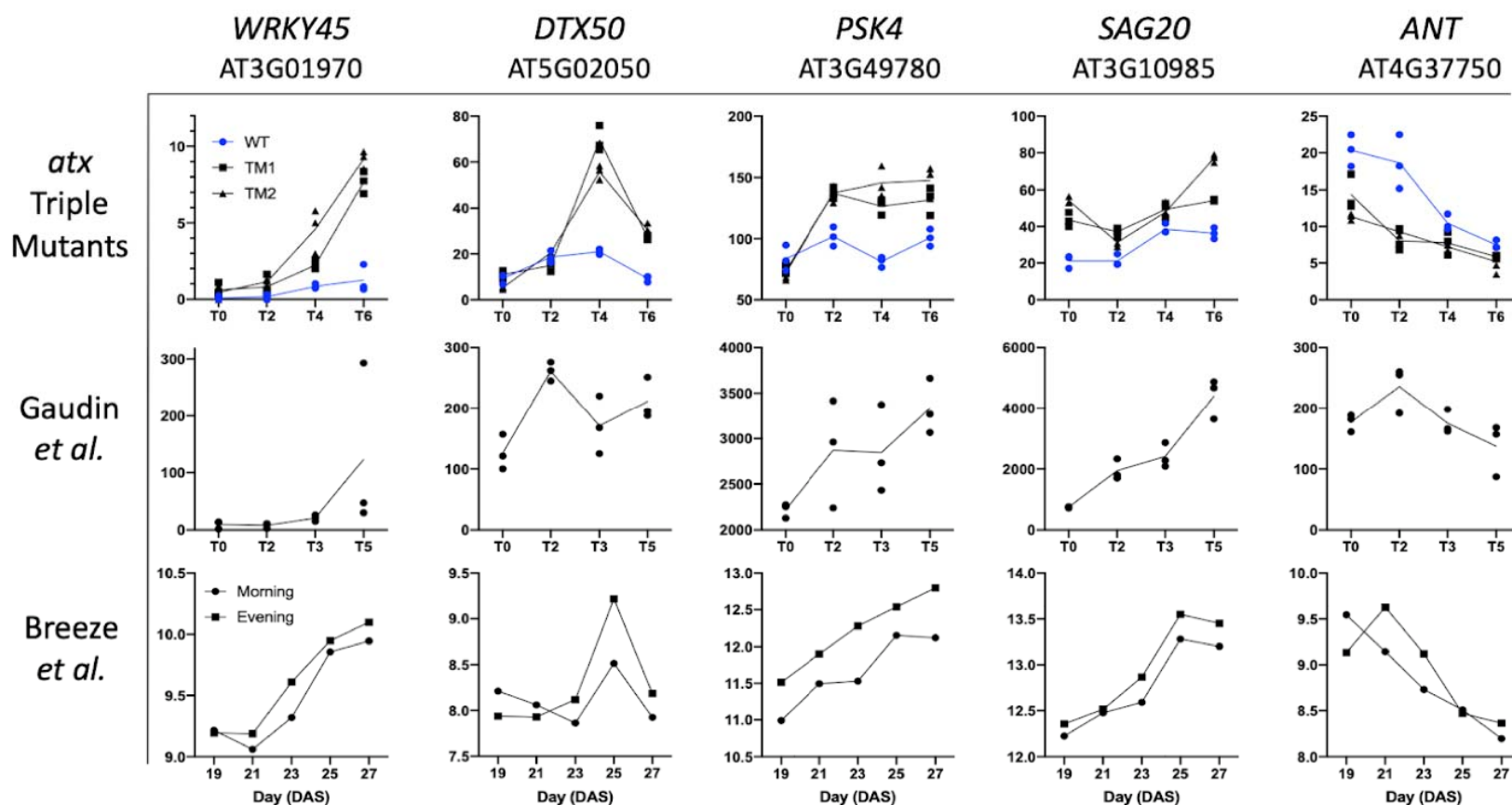
Figure 5: Examples of BAG Expression Across Experiments

Raw data from each experiment were used to generate these graphs in GraphPad PRISM. Data from the *atx* TM and Gaudin *et al.* experiments represent FPKM from RNA-seq, while Breeze *et al.* is Lowess normalized averaged (4 reps) signals in log space from a microarray experiment. Bolting occurs at T0 in the *atx* TM experiment and at Day 21 in the Breeze *et al.* experiment. T0 in the Gaudin *et al.* experiment represents the time of photoperiodic transition from short day to long day conditions. Samples from plants undergoing the vegetative-reprodutive transition are shown in black while vegetative control plants are shown in blue.
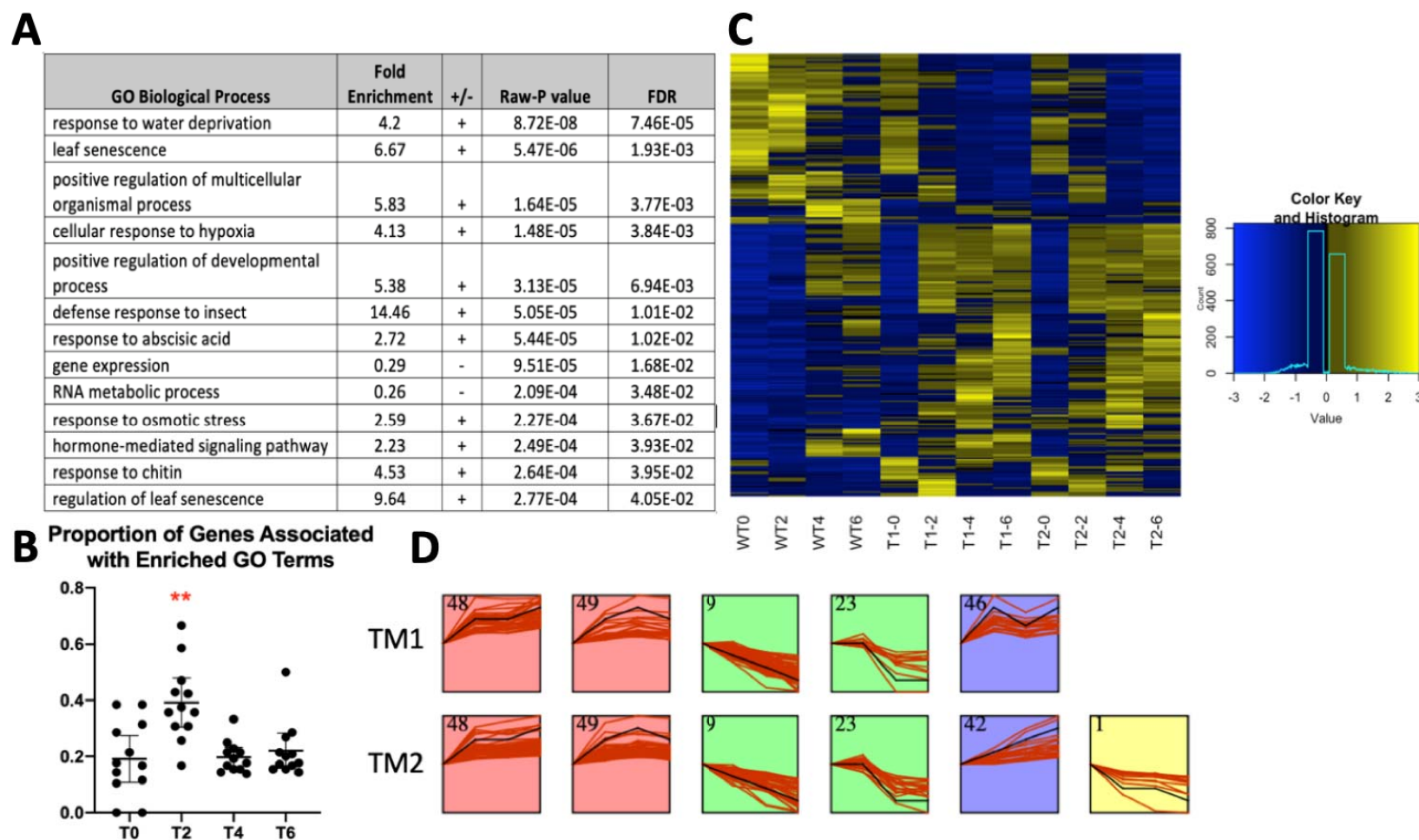
A

GO Biological Process	Fold Enrichment	+/-	Raw-P value	FDR
response to water deprivation	4.2	+	8.72E-08	7.46E-05
leaf senescence	6.67	+	5.47E-06	1.93E-03
positive regulation of multicellular organismal process	5.83	+	1.64E-05	3.77E-03
cellular response to hypoxia	4.13	+	1.48E-05	3.84E-03
positive regulation of developmental process	5.38	+	3.13E-05	6.94E-03
defense response to insect	14.46	+	5.05E-05	1.01E-02
response to abscisic acid	2.72	+	5.44E-05	1.02E-02
gene expression	0.29	-	9.51E-05	1.68E-02
RNA metabolic process	0.26	-	2.09E-04	3.48E-02
response to osmotic stress	2.59	+	2.27E-04	3.67E-02
hormone-mediated signaling pathway	2.23	+	2.49E-04	3.93E-02
response to chitin	4.53	+	2.64E-04	3.95E-02
regulation of leaf senescence	9.64	+	2.77E-04	4.05E-02

C

B Proportion of Genes Associated with Enriched GO Terms

D

Figure 6: Bolting Associated Genes (BAGs)

A: Enriched GO terms from a Panther Gene Ontology analysis are shown. B. An ANOVA run on the time-intersected enriched BAGs generated a significant P-value (1.29569E-05). Pairwise T-tests were then completed using a Bonferonni corrected p-value (0.05/6 = 0.0083), which indicated that T2 was significantly different than all other time points [p= 0.000303 (T0), 0.000154 (T4), 0.000825 (T6)]. No other significant results were detected. Error bars show the 95 percent confidence intervals. C: A heatmap showing BAG expression levels in all 12 transcriptomes was generated in R. D. Short Time Series Expression Miner (STEM) was used to find significant clusters of gene expression changes.

A
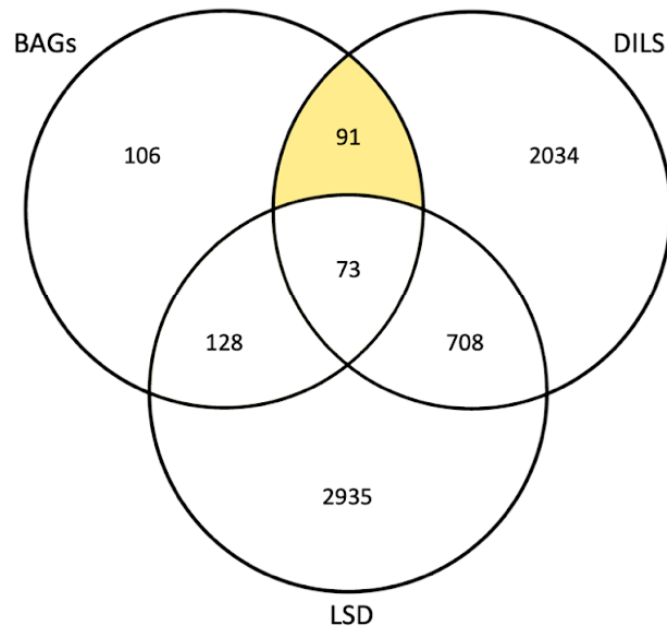
B

Gene ID	Bolting	DILS	Gene Symbol/Description
AT1G13930	Up	Down	Involved in response to salt stress
AT1G33260	Up	Down	Protein kinase superfamily protein
AT1G48480	Down	Down	RECEPTOR-LIKE KINASE 1 (RKL1)
AT1G54820	Down	Down	Protein kinase superfamily protein
AT1G62570	Up	Up	(FMO GS-OX4)
AT1G64670	Down	Down	BODYGUARD1 (BDG1)
AT1G68570	Up	Down	NRT1/ PTR FAMILY 3.1 (NPF3.1)
AT1G72800	Up	Up	RNA-binding (RRM/RBD/RNP motifs) family protein
AT1G74930	Down	Down	(ORA47)
AT2G26870	Down	Down	NON-SPECIFIC PHOSPHOLIPASE C2 (NPC2)
AT2G34510	Down	Down	(ATHB-1)
AT2G40960	Down	Down	Single-stranded nucleic acid binding R3H protein
AT2G42380	Down	Down	(BZIP34)
AT3G01480	Down	Down	CYCLOPHILIN 38 (CYP38)
AT3G12610	Down	Down	DNA-DAMAGE REPAIR/TOLERATION 100 (DRT100)
AT3G17840	Down	Down	RECEPTOR-LIKE KINASE 902 (RLK902)
AT3G19820	Down	Down	DWARF 1 (DWF1)
AT3G22120	Down	Down	CELL WALL-PLASMA MEMBRANE LINKER PROTEIN (CWLP)
AT3G22750	Up	Up	Protein kinase superfamily protein
AT3G51860	Up	Up	CATION EXCHANGER 3 (CAX3)
AT4G34760	Down	Down	SMALL AUXIN UPREGULATED RNA 50 (SAUR50)
AT4G38770	Down	Down	PROLINE-RICH PROTEIN 4 (PRP4)
AT5G02190	Down	Down	PROMOTION OF CELL SURVIVAL 1 (PCS1)
AT5G02760	Down	Down	ARABIDOPSIS PP2C CLADE D 7 (APD7)
AT5G15230	Down	Down	MATERNAL EFFECT EMBRYO ARREST 3 (MEE3)
AT5G15230	Down	Down	GAST1 PROTEIN HOMOLOG 4 (GASA4)
AT5G18060	Down	Down	SMALL AUXIN UP RNA 23 (SAUR23)
AT5G20630	Down	Down	GERMIN 3 (GER3)
AT5G22580	Down	Down	Stress responsive A/B Barrel Domain-containing protein
AT5G26000	Down	Down	THIOGLUCOSIDE GLUCOHYDROLASE 1 (TGG1) (BGLU38)
AT5G57180	Down	Down	CHLOROPLAST IMPORT APPARATUS 2 (CIA2)

Figure 7: Potential Novel LS Regulators

The Venn Diagram shows overlap between the 398 BAGs, the 2906 DEGs from the DILS dataset, and the 3844 SAGs in the Leaf Senescence Database (LSD) (CITE 2019). The 91 BAGs that were differentially expressed in the DILS dataset but not in the LSD are highlighted. Select signaling genes are shown in the table along with their direction of gene expression at bolting and during DILS. Gene Symbols/Descriptions were obtained using the bulk data retrieval tool in TAIR.
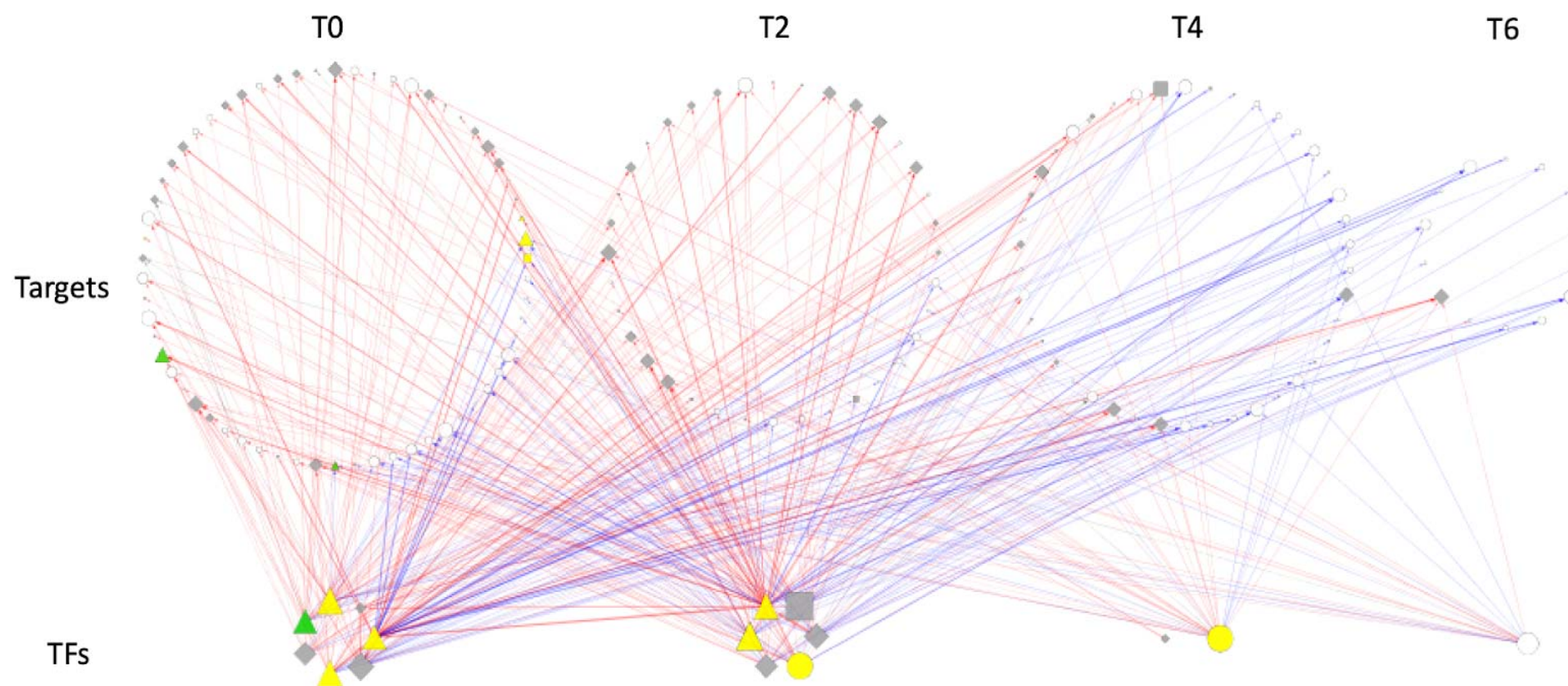
Figure 8: Bolting Time-Associated Gene Regulatory Network
The network was manually constructed as described in the Methods, and uploaded to Cytoscape for visualization. White nodes were not present in the LSD. Grey nodes were present, but had an unclear function listed in the LSD. Yellow nodes promote LS while green nodes prevent LS. Upregulation is shown by red edges and downregulation is shown with blue edges. Node shape refers to the type of evidence used to determine LS association in LSD 3.0; diamonds represent genomic (microarray) data, triangles represent mutant studies, and squares represent molecular data.
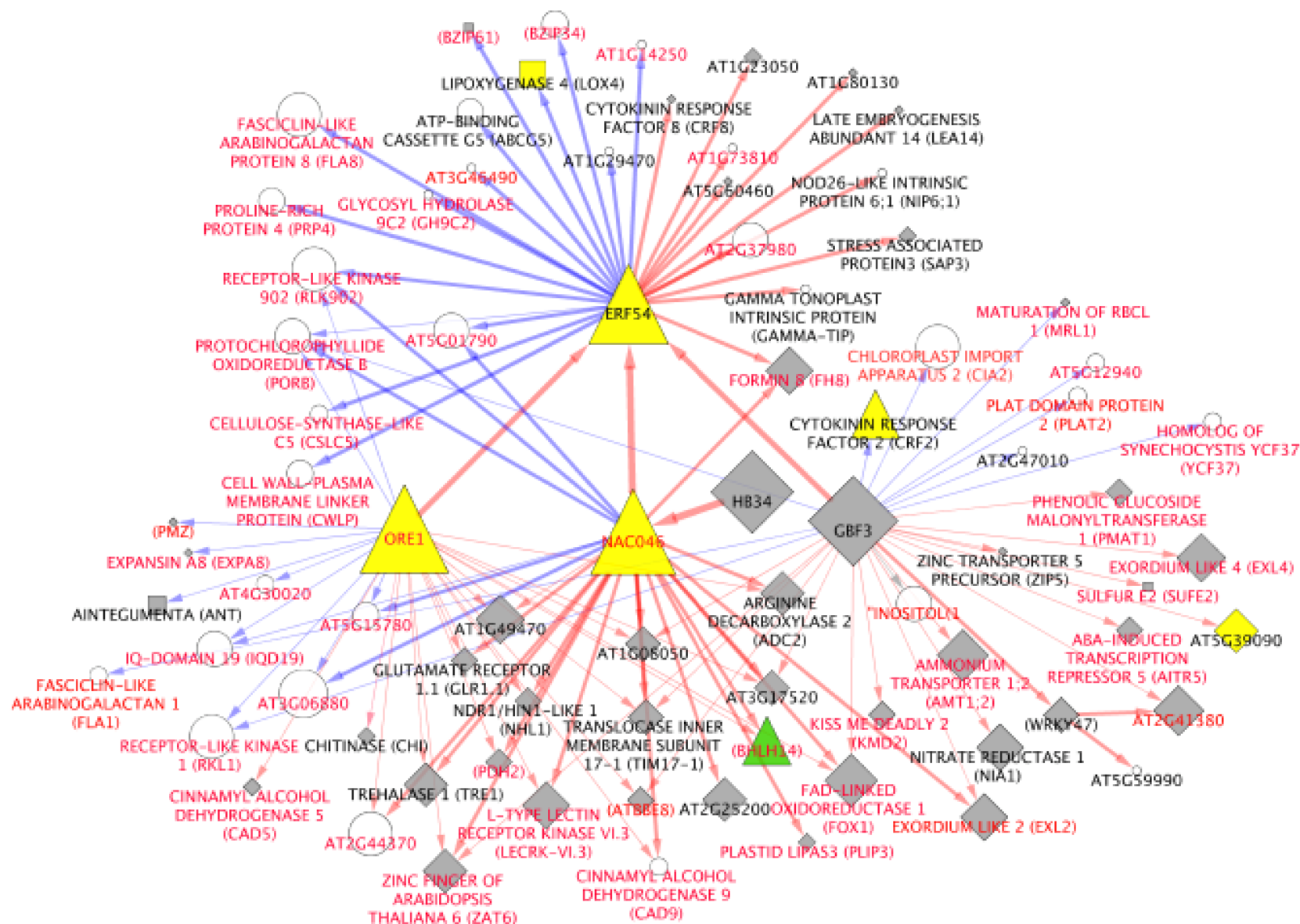
Figure 9: *ERF054* Subnetwork

White nodes were not present in the LSD. Grey nodes were present, but had an unclear function. Yellow nodes promote LS while green nodes prevent LS. Upregulation is shown by red edges and downregulation is shown with blue edges. Node shape refers to the type of evidence used to determine LS association; diamonds represent genomic data, triangles represent mutant studies, and squares represent molecular data. Red labels refer to genes that are differentially expressed during DILS and black genes were not differentially expressed during DILS. Potential novel LS regulators are shown as white nodes with red labels.
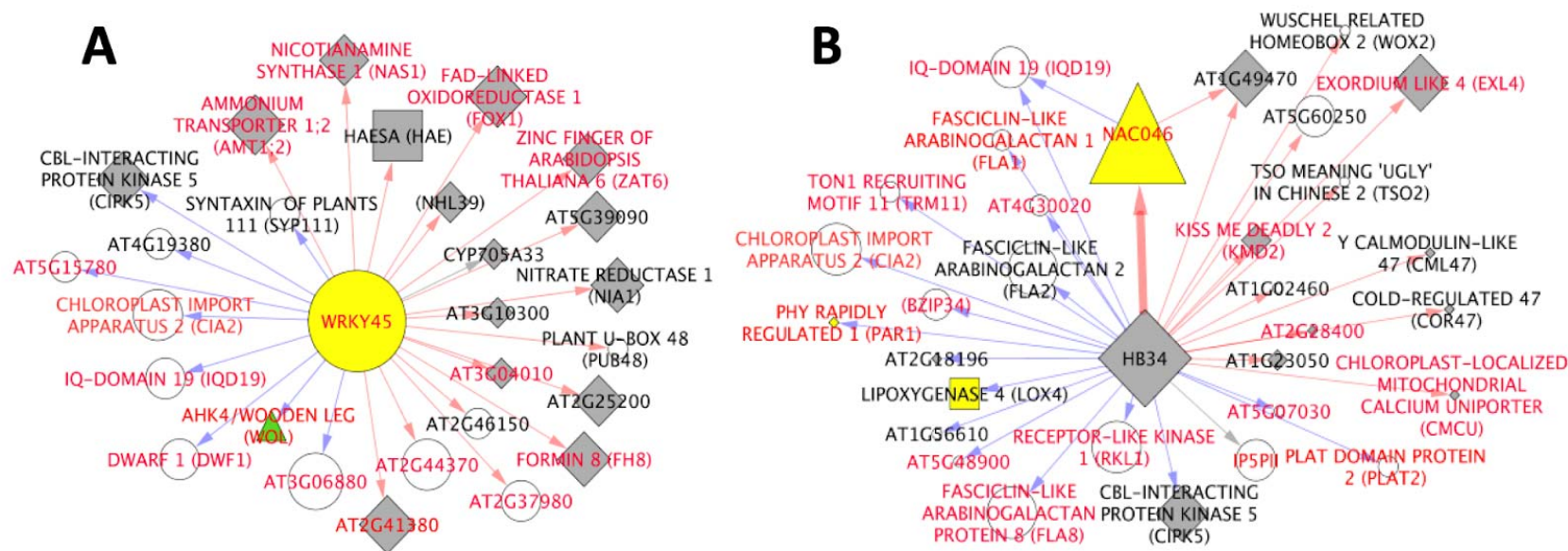
Figure 10: Select Subnetworks

The network was manually constructed in R (description in methods), then uploaded to Cytoscape for visualization. White nodes were not present in the LSD. Grey nodes were present, but had an unclear function. Yellow nodes promote LS while green nodes prevent LS. Upregulation is shown by red edges and downregulation is shown with blue edges. Node shape refers to the type of evidence used to determine LS association; diamonds represent genomic data, triangles represent mutant studies, and squares represent molecular data.